Plan of Lectures

- Early structure formation & Reionization: possible observational signatures
- Large scale structure of the universe: large scale motions - QSO spectra
- Non-standard cosmological models: dark energy from geometry - physics of dark matter - cosmology with no dark matter

The dark night: Olbers' paradox

Refs: Harrison E., *cosmology*, 1980 ; Wesson P. S., ApJ. 1991

Why is the sky dark at night?

Olbers' paradox

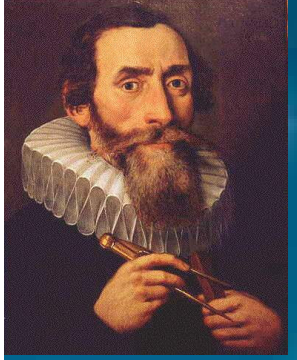

Johannes Kepler
(1571-1630)

Assuming identical stars and Euclidean space:

$$I = \sum_i \frac{FA}{4\pi r_i^2} = \frac{F}{4\pi} \sum_i \Omega_i = F$$

$\Rightarrow$ an awfully bright night!

F = total light emitted by a star per unit surface area
A = area of a star
r_i = distance of a star
I = flux of light reaching Earth

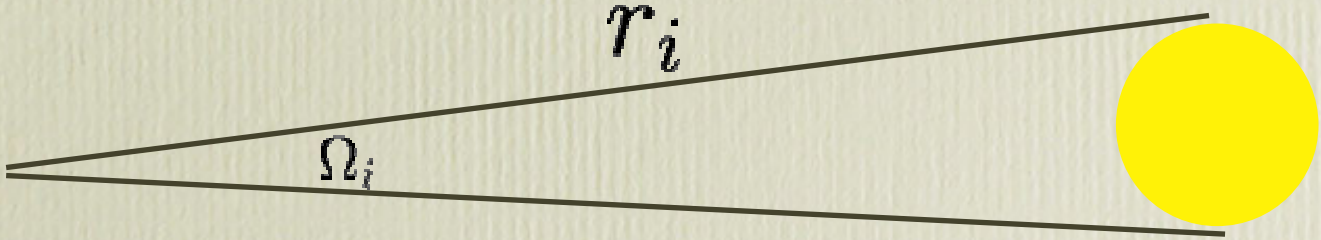

Ideas:

- dust obscuration: does not work
- the expansion of the universe: helps
- a fractal distribution of stars
- stars do not exist beyond a limiting distance: this is basically the answer

a fractal distribution

THE UNIVERSE IS NOT A FRACTAL

Ideas:

- dust obscuration: does not work
- the expansion of the universe: helps
- a fractal distribution of stars
- stars do not exist beyond a limiting distance: this is basically the answer. This solution naturally fits in modern cosmology.

Emergence of luminous structures in the Universe

- pre-recombination. the bottleneck is the *huge Jeans mass*
- linear fluctuations: Dark Ages: neutral hydrogen. The bottleneck is *lack of non-linear dense regions*
- non-linear growth of fluctuations ⇒ onset of galaxy formation ⇒ hydrogen reionization. The bottleneck is *cooling*.

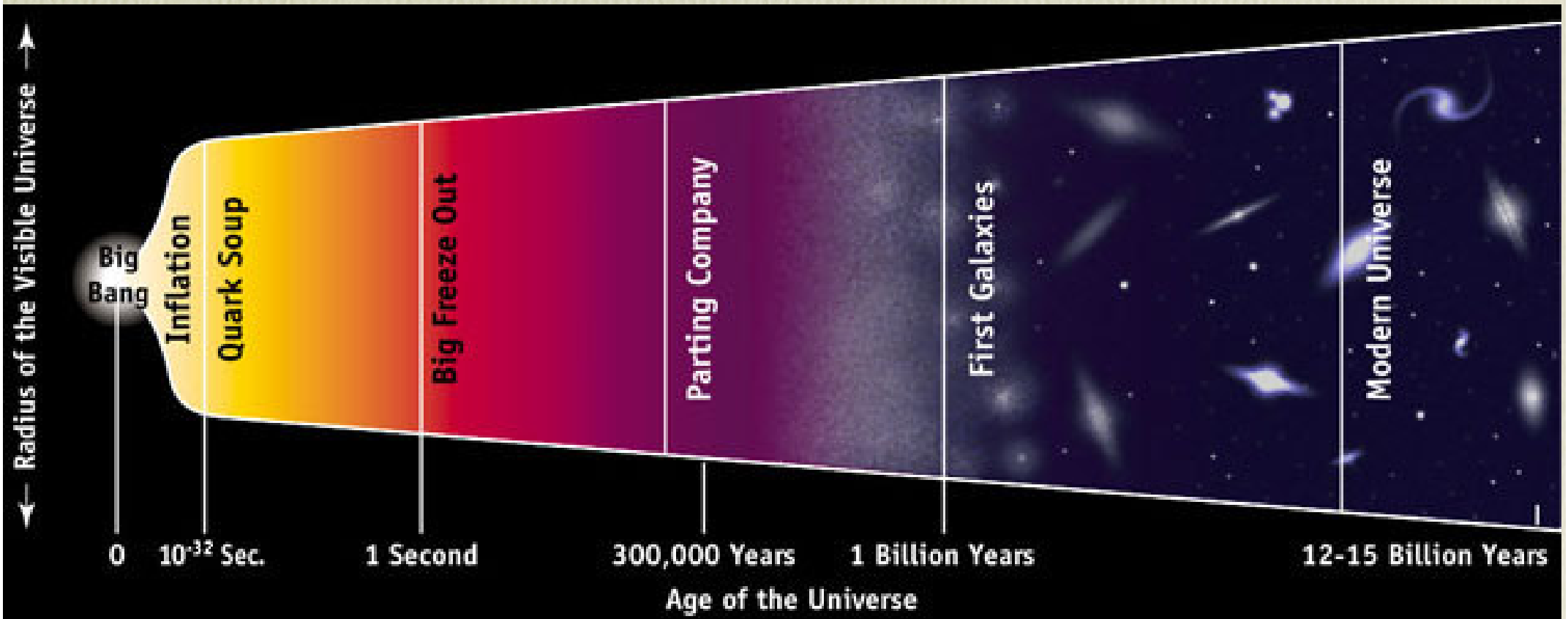

Reionization of hydrogen is the least understood stage in the evolution of our Univese.

The most direct observational illustration of hydrogen reionization is the spectra of high redshift QSOs.

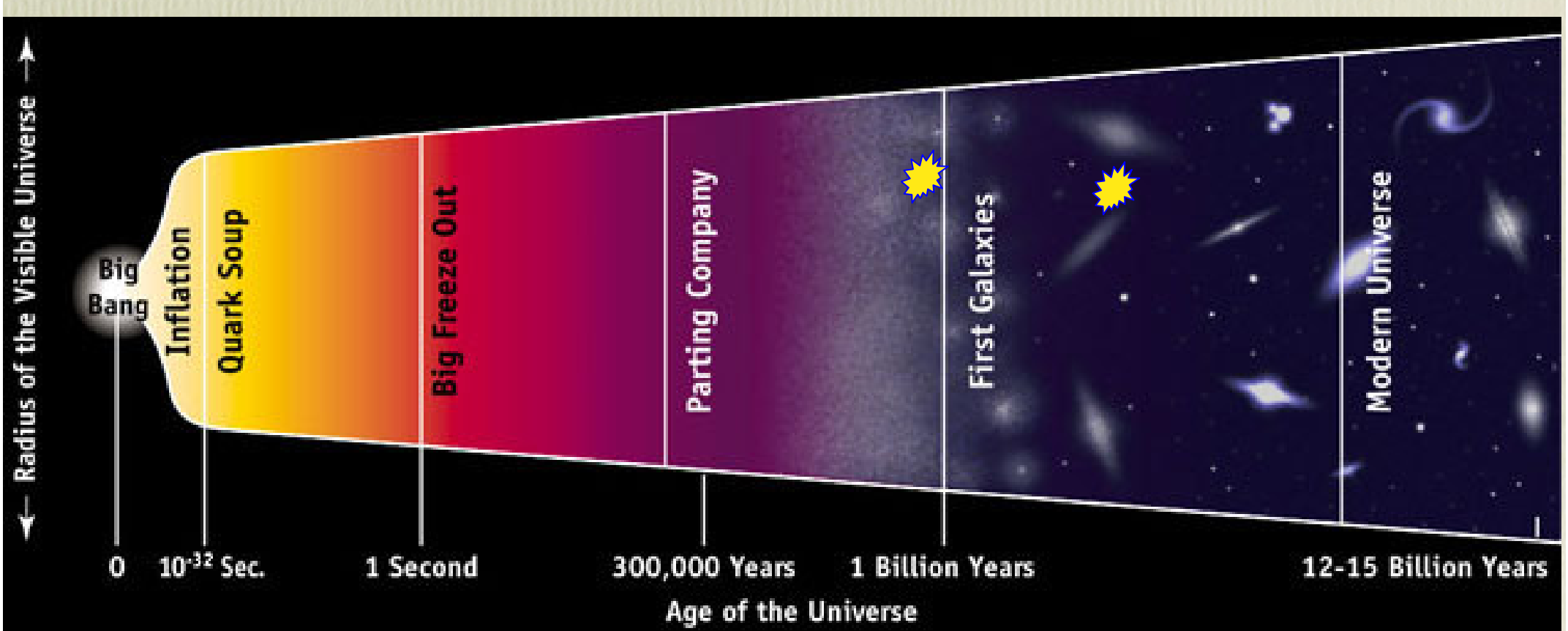

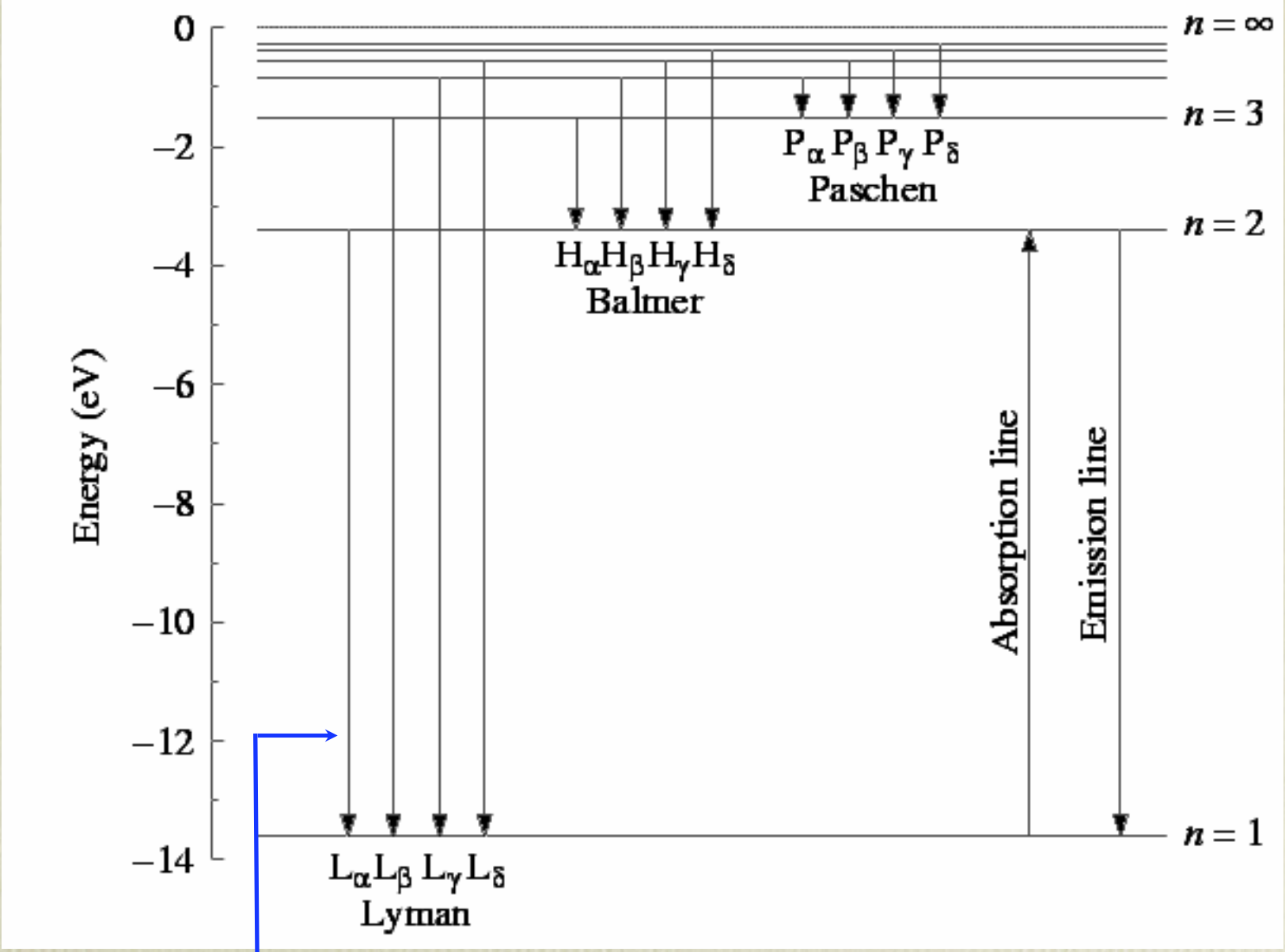

$\lambda_\alpha \approx 1216\mathring{A}$ or $h\nu \approx 10.2$eV

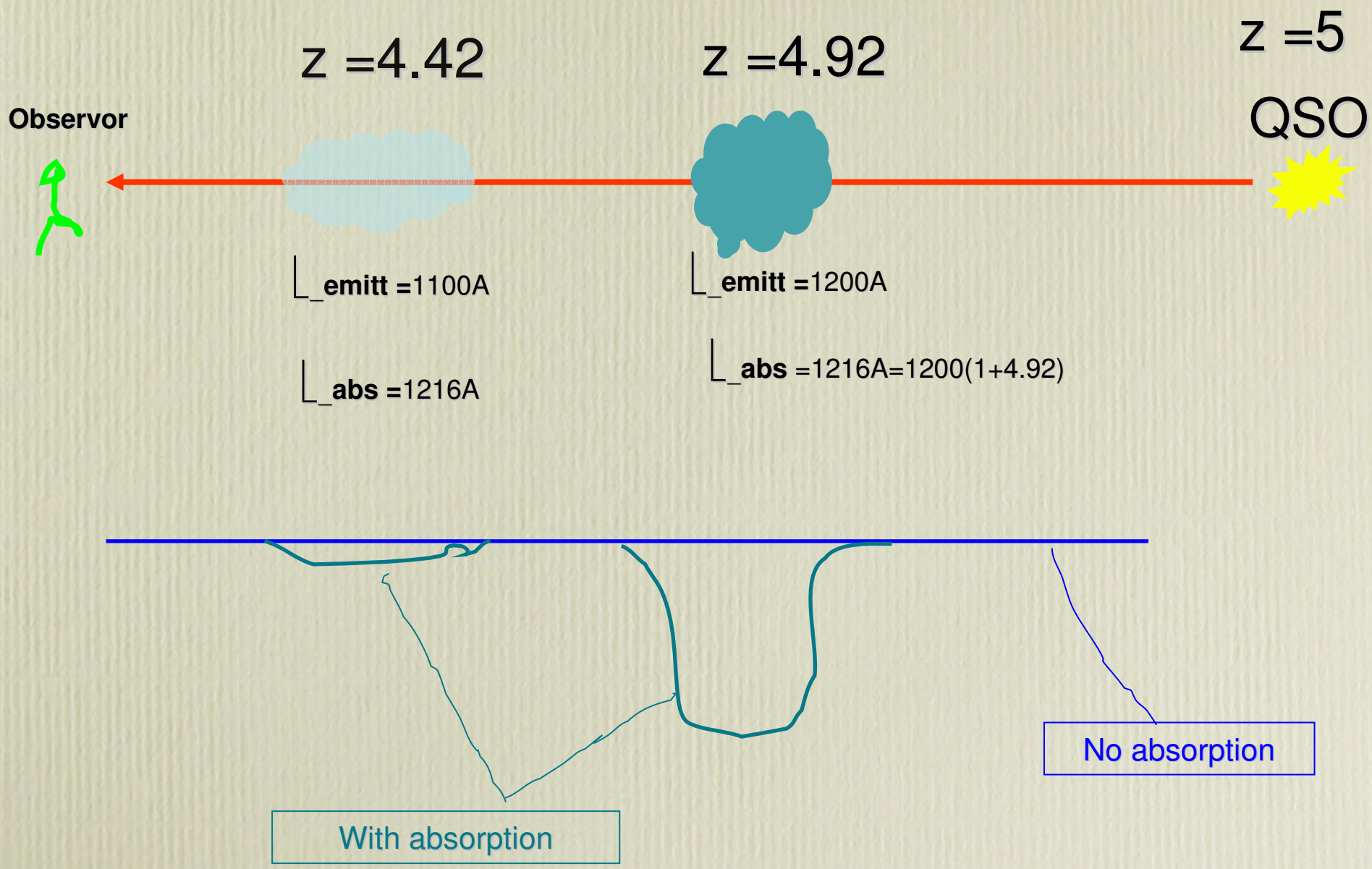
z =4.42
z =4.92
z =5
Observor
QSO
emitt =1100A
emitt =1200A
abs =1216A
abs =1216A=1200(1+4.92)
With absorption
No absorption

H$_I$ number density (simulation by B. Ciardi)

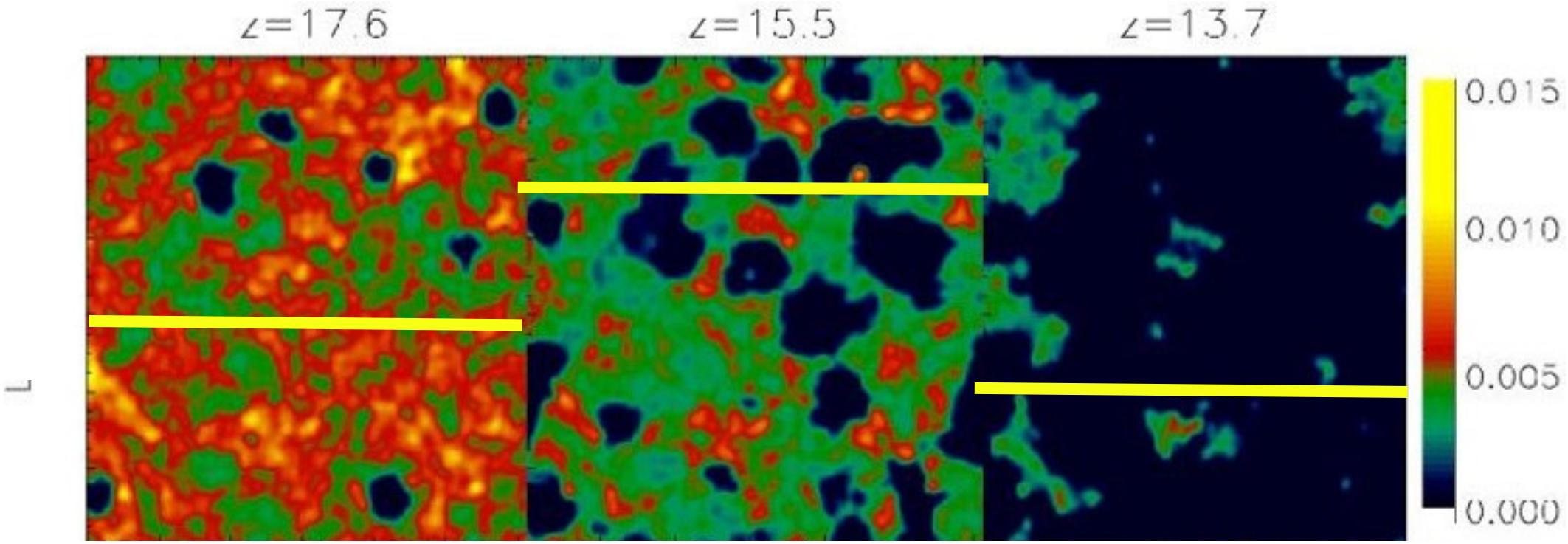

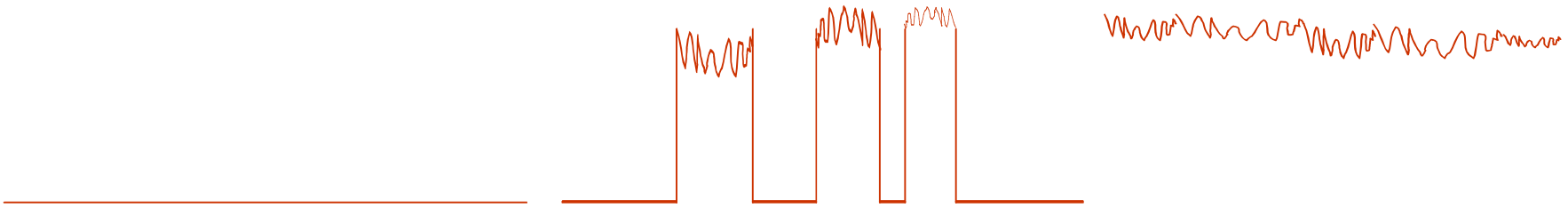

full absorption

The QSO situation

Becker *et.al 2002*

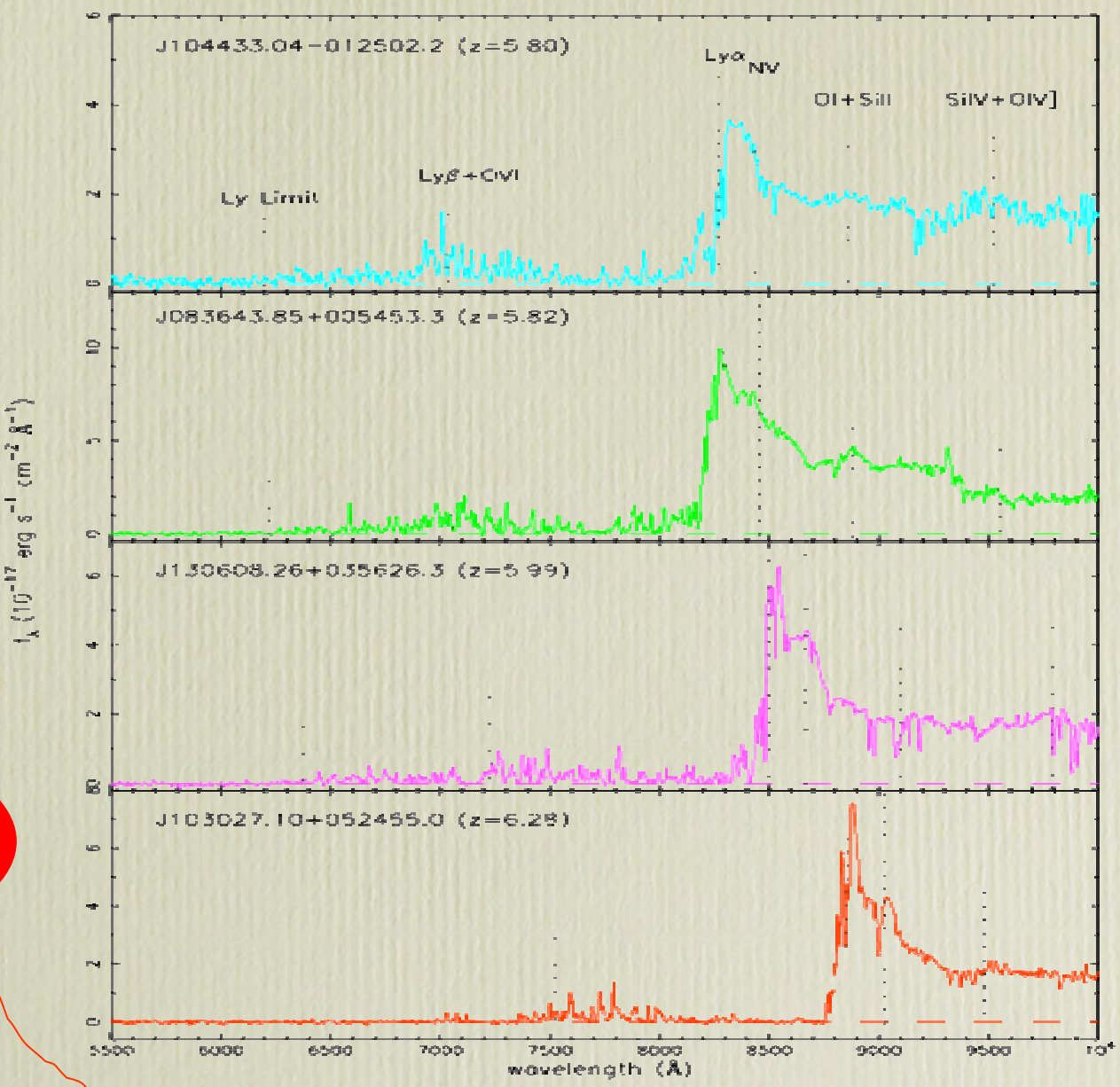

~60Mpc/h region with large optical depth!!!

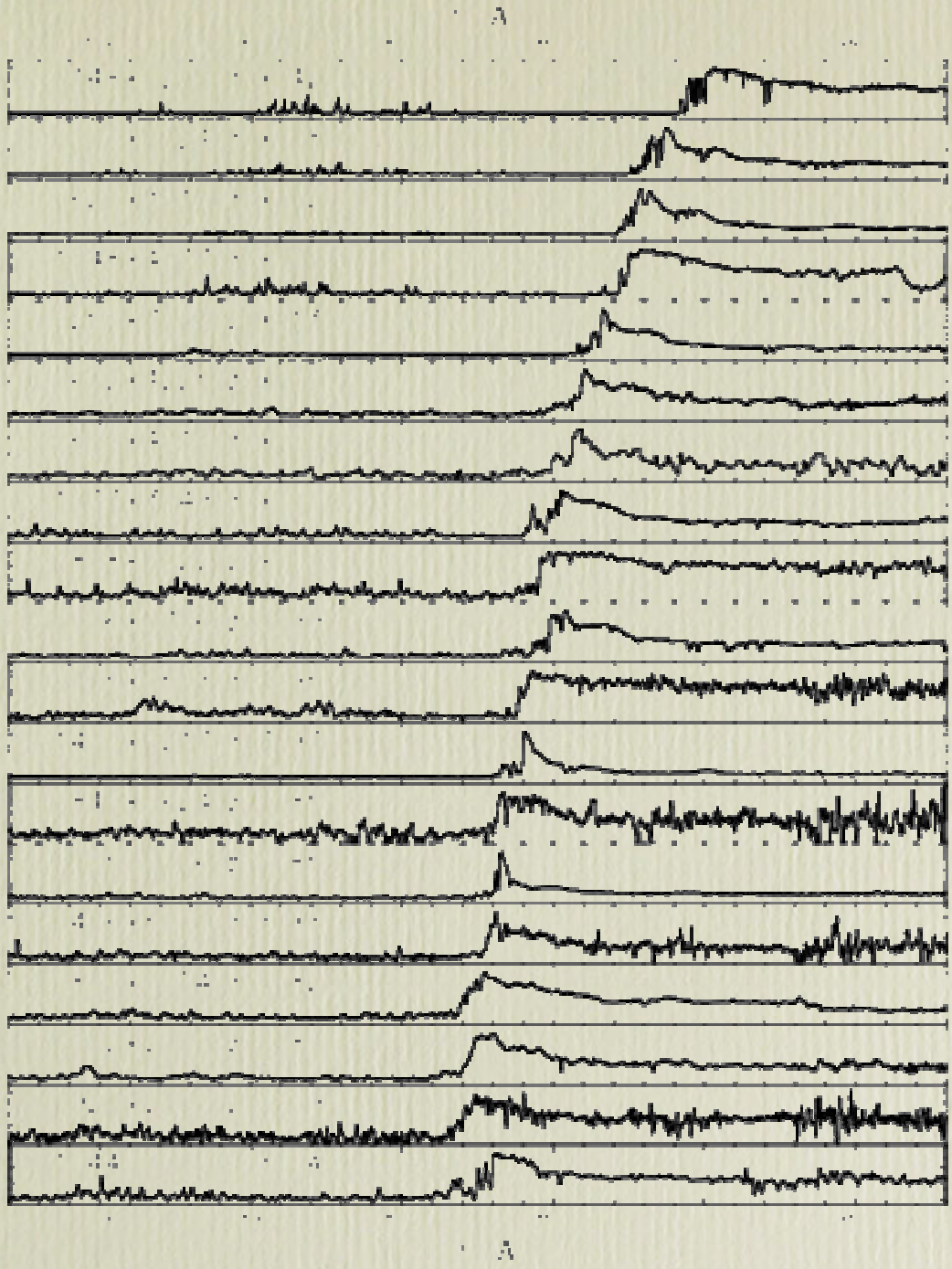

Fig. 1. Spectra of our sample of nineteen SDSS quasars at $5.74 < z < 6.42$. Twelve of the spectra were taken with Keck/ESI, while the others were observed with the MMT/Red Channel and Kitt Peak 4-meter/MARS spectrographs. See Table 1 for detailed information.

Xiaohui Fan,[1] Joseph F. Hennawi,[2] Gordon T. Richards,[3] Michael A. Strauss,[4] Donald P. Schneider,[5] Jonathan L. Donley,[1] Jason E. Young,[1] James Annis,[6] Huan Lin,[6] Robert Lupton,[4] Robert H. Lupton,[4] James E. Gunn,[4] Gillian R. Knapp,[4] W. N. Brandt,[5] Scott Anderson,[7] Neta A. Bahcall,[4] Jon Brinkmann,[8] Robert J. Brunner,[9] Masataka Fukugita,[10] Alexander S. Szalay,[11] Gyula P. Szokoly,[12] and Donald G. York[13]

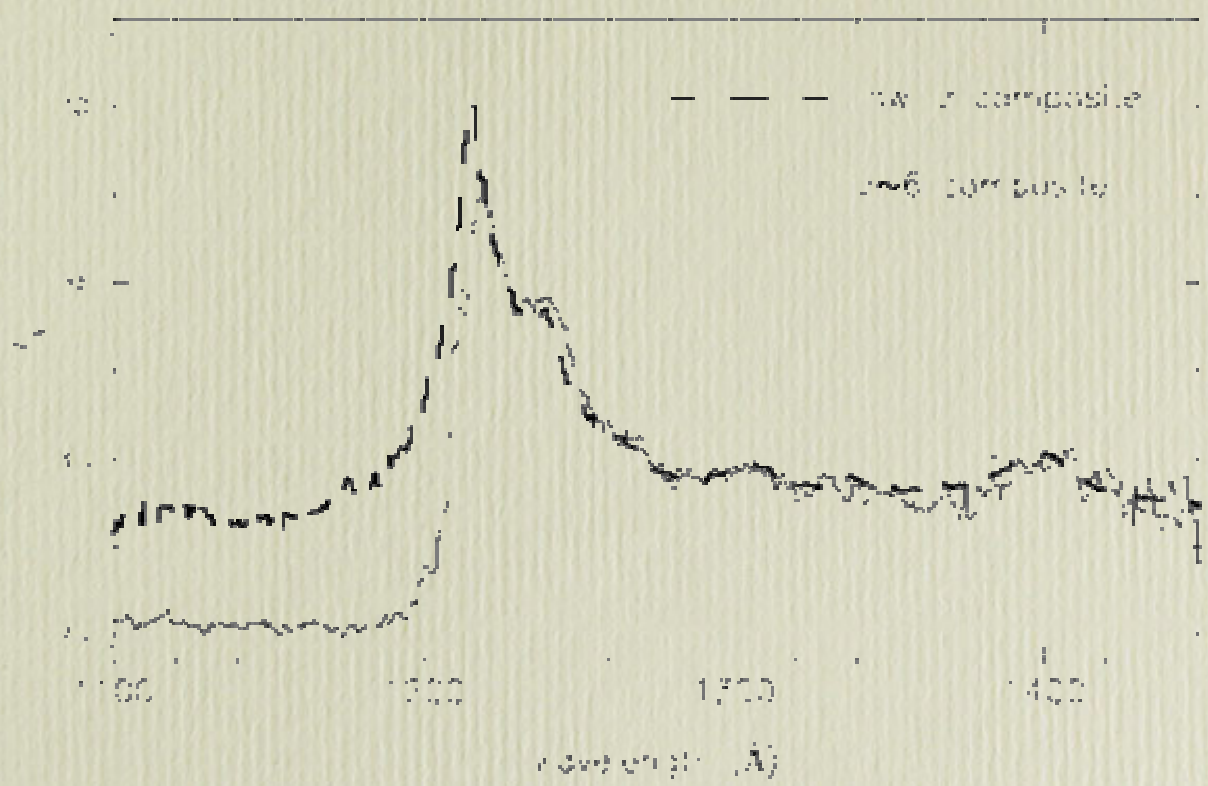

FIG. 3.—Composite spectrum of 11 $z \sim 6$ quasars (*solid line*). The spectrum of SDSS J0005−0002 was not included because of its low S/N. The spectrum of each quasar is redshifted, scaled according to its m_{1450} magnitude, and averaged with equal weighting. For comparison, we also plot the low-redshift quasar spectral composite from Vanden Berk et al. (2001). The effective redshift in the 1000–1500 Å range in the Vanden Berk et al. composite is about 2. The quasar intrinsic spectrum redward of Lyα emission shows no detectable evolution up to $z \sim 6$, in terms of both the continuum shape and emission-line strengths. On the blue side of Lyα emission, the strong IGM absorption at $z \sim 6$ removes most of the quasar flux.

The formation of a galaxy

expansion

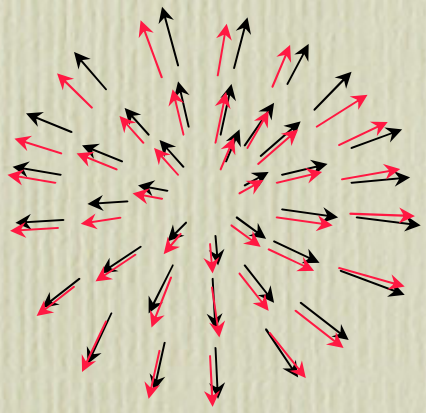

collapse

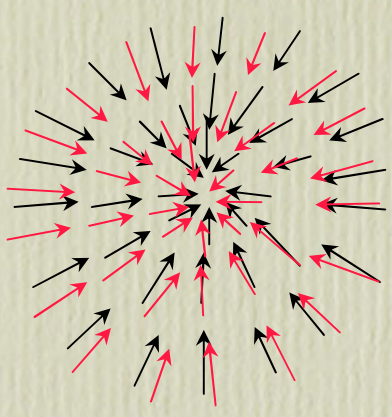

shock heating to T_vir

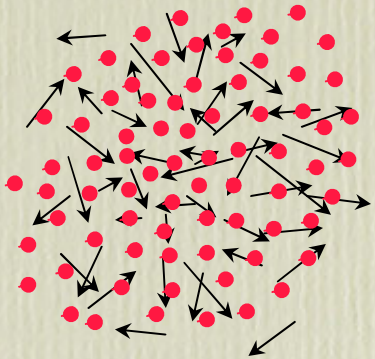

cooling without angular momentum

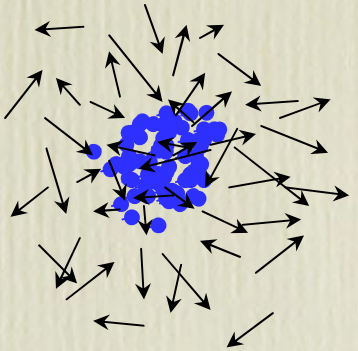

$$T_{\rm vir} = 2 \times 10^{4}{\rm K} \left(\frac{M_{\rm halo}}{10^{8} h^{-1} M_{\odot}}\right)^{2/3} \left(\frac{1+z}{10}\right)$$

star formation

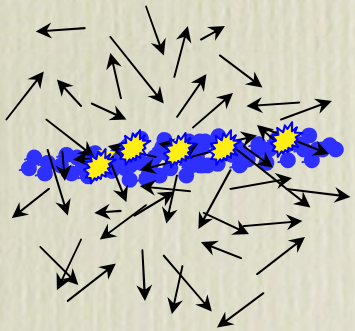

cooling with angular momentum

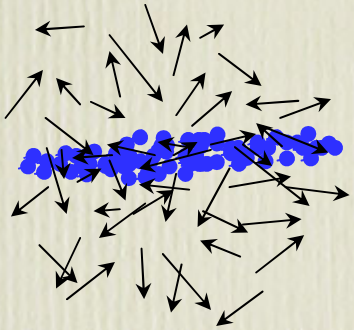

Dynamics of gas and collisionless dark matter

Euler:

$$\frac{\mathrm{d}\mathbf{v}_{\mathrm{gas}}}{\mathrm{d}t} = -\frac{\nabla p}{\rho_{\mathrm{gas}}} - \nabla\Phi$$

Continuity:

$$\frac{\mathrm{d}\rho_{\mathrm{gas}}}{\mathrm{d}t} = -\nabla \cdot \mathbf{v}_{\mathrm{gas}}$$

Poisson:

$$\nabla^2\Phi = 4\pi G(\rho_{\mathrm{dm}} + \rho_{\mathrm{gas}})$$

The energy equation:

$$\frac{\mathrm{d}T_{\mathrm{gas}}}{\mathrm{d}t} = \frac{2}{3}\frac{T_{\mathrm{gas}}}{\rho_{\mathrm{gas}}}\frac{\mathrm{d}\rho}{\mathrm{d}t} - C$$

cooling.

Cooling Channels for Metal Free Gas

- cooling down to 10^4 K°
  - Compton cooling
  - atomic cooling
  - free-free cooling
- cooling down to ~ 100 K°
  - molecular cooling

Compton Cooing: coupling of the CMBR to residual photons

Refs: Peebles, 1993, *principles of physical cosmology*

Consider an electron moving at $v \ll c$ through the CMBR. In the frame of the electron, the temperature of photons moving towards the electron at angle θ is (basically Doppler effect),

$$T(\theta) = T_0(1 + \frac{v}{c}\cos\theta)$$

The momentum flux hitting the electron through a solid angle $\mathrm{d}\omega$ in the direction θ is $a_B T(\theta)^4/c\,\mathrm{d}\omega$. The rate of transfer of this momentum is $\sigma_t a_B T(\theta)^4/c\,\mathrm{d}\omega$. Integrating over all directions gives the total force on the electron

$$F = \frac{4}{3}\frac{v}{c}\sigma_t a_B T_0^4 \ .$$

For thermal electrons, $(3/2)kT_e = (1/2)m_e < v^2 >$, the rate of energy transfer per electron is

$$\frac{\mathrm{d}}{\mathrm{d}t}\left(\frac{1}{2}m_e < v^2 >\right) = \frac{\mathrm{d}}{\mathrm{d}t}\left(\frac{3}{2}kT_e\right) =< Fv >$$

This energy loss must be shared with atoms and protons. If $n_e = n_p = x_e(n_p + n_H)$ then the final expression is

$$\boxed{\frac{\mathrm{d}T_e}{\mathrm{d}t} = \frac{x_e}{1+x_e}\frac{8\sigma_t a_B T_0^4}{3m_e c}(T_0 - T_e)}$$

where heating by CMBR is now included.

This expression is independent of density! For $x_e = 1$ we get efficient cooling until $z \sim 10$. As $T_e \Rightarrow 10^4$ K, the ionized fraction $x_e \Rightarrow 0$ Compton cooling becomes inefficient.

Atomic Cooling

Refs: Sutherland & Dopota. 1983. AJ

This also is good only for $T > 10^4$ K. For $T \lesssim 10^{5.6}$ K cooling is dominated by collisional excitations of hydrogen and helium. At $T > 10^{5.6}$ K it is dominated by bremsstrahlung (free-free) radiation.

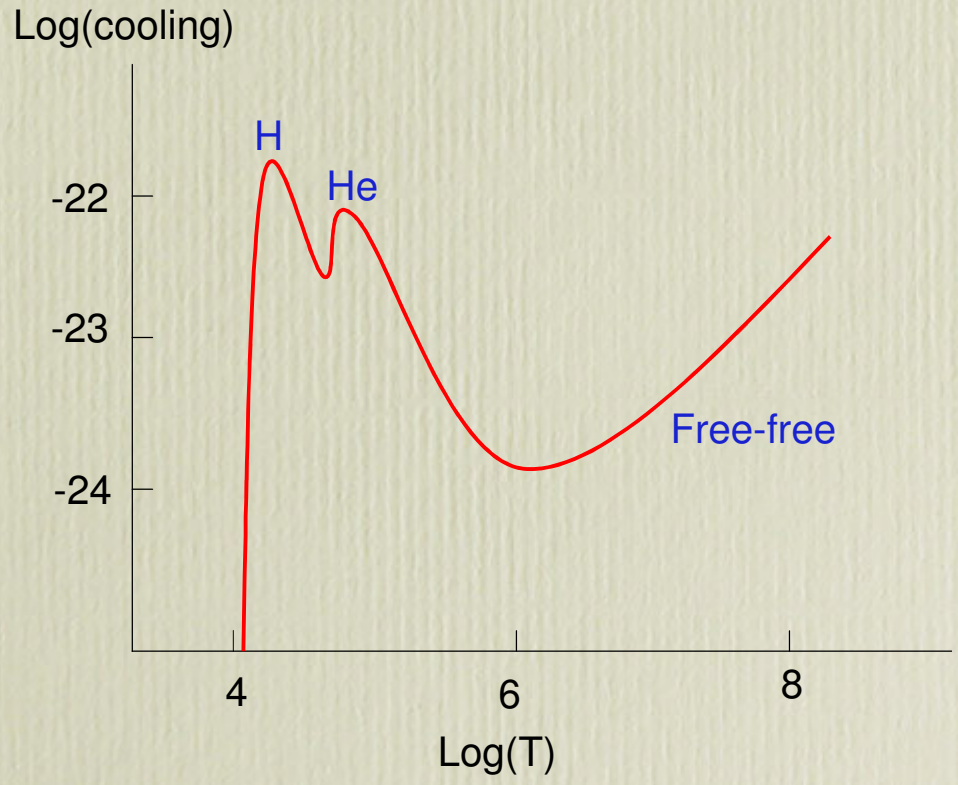

Molecular Cooling

Refs: Yoshida, Abel, Hernquist, Sugiyama, 2003, ApJ; Tegmark, Silk, Rees, Blanchard, Abel, 1997, ApJ

Cooling by radiative decay of rotationally or vibrationally excited H_2 molecule.

The problem is the formation of H_2. At the relevant redshifts, H_2 forms through the channel:

$$H + e \longleftrightarrow H^- + \gamma$$

$$H^- + H \longleftrightarrow H_2 + e$$

Free electrons are needed!

In the most elementary scenario and certainly the one valid for first generation of forming stars, free electrons are provided as leftover from the pre-recombination era.

The fraction of leftover electrons is $x_e \sim 3 \times 10^{-5}$.
That is sufficient!

Yoshida, Abel, Hernquist, Sugiyama, 2003,

simulation at z=17

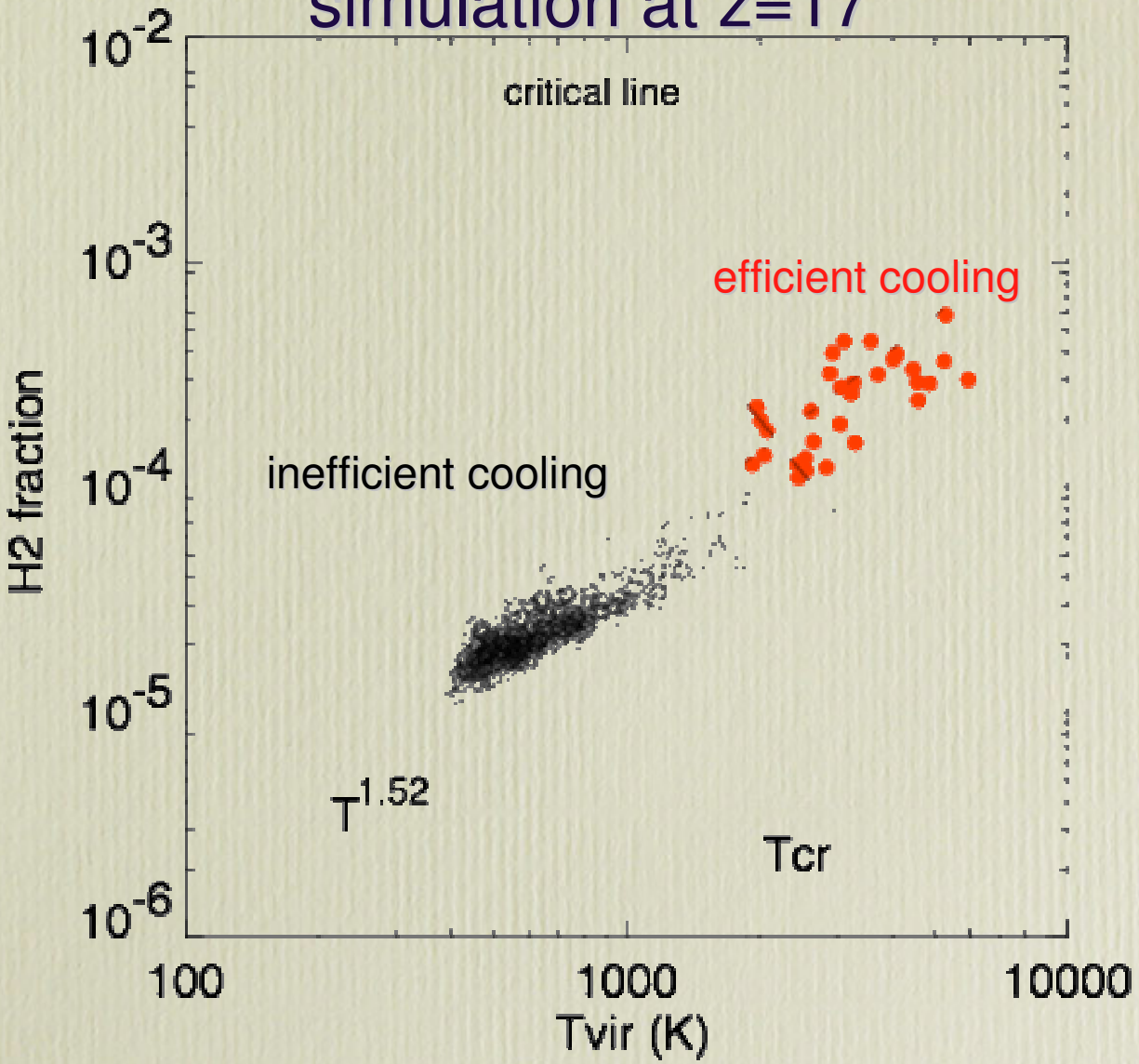

$$T_{\rm vir} = 2 \times 10^4 {\rm K} \left(\frac{M_{\rm halo}}{10^8 h^{-1} M_\odot} \right)^{2/3} \left(\frac{1+z}{10} \right)$$

Do we need H_2 cooling?

Without H_2, only halos with $T_{\rm vir} > 10^4 K$ can cool. No problem to reionize the universe at $z \gtrsim 6$ or so for reasonable recipes of star/galaxy formation.

Reionization at $z \sim 6$ is consistent with QSO spectra.

But WMAP implies some reionization at earlier times $\Rightarrow$ H_2 maybe needed at higher redshifts. We will get back to this point soon.

Reionization by UV photons emitted stars

The ionization threshold of H_I is 13.6 eV, corresponding to 912 $\mathring{A}$. Stars emit a lot of UV photons with wavelengths shorter than 912 $\mathring{A}$.

"Realistic" Modeling of Reionization by UV

- "reasonable" initial conditions:
  - a concordance model √√
  - exploration of alternative models ××
- growth of mass density perturbations √√√
- star formation recipe at high redshift ×××× ×××× ×××× ××××
- amount of UV radiation emitted from stars √√
- amount of UV radiation that actually manages to leave the galaxy into the intergalactic medium (IGM) ××
- the propagation of radiation in the IGM:
  - numerical radiative transfer √
  - small simulation box ××
- "back-reaction" of reionization on star/galaxy formation ××

UV ionization fronts around individual sources

$$l_{\rm pl.} = 0.3(1 - x_e)(1 + z)^{-3}\,{\rm Mpc}$$

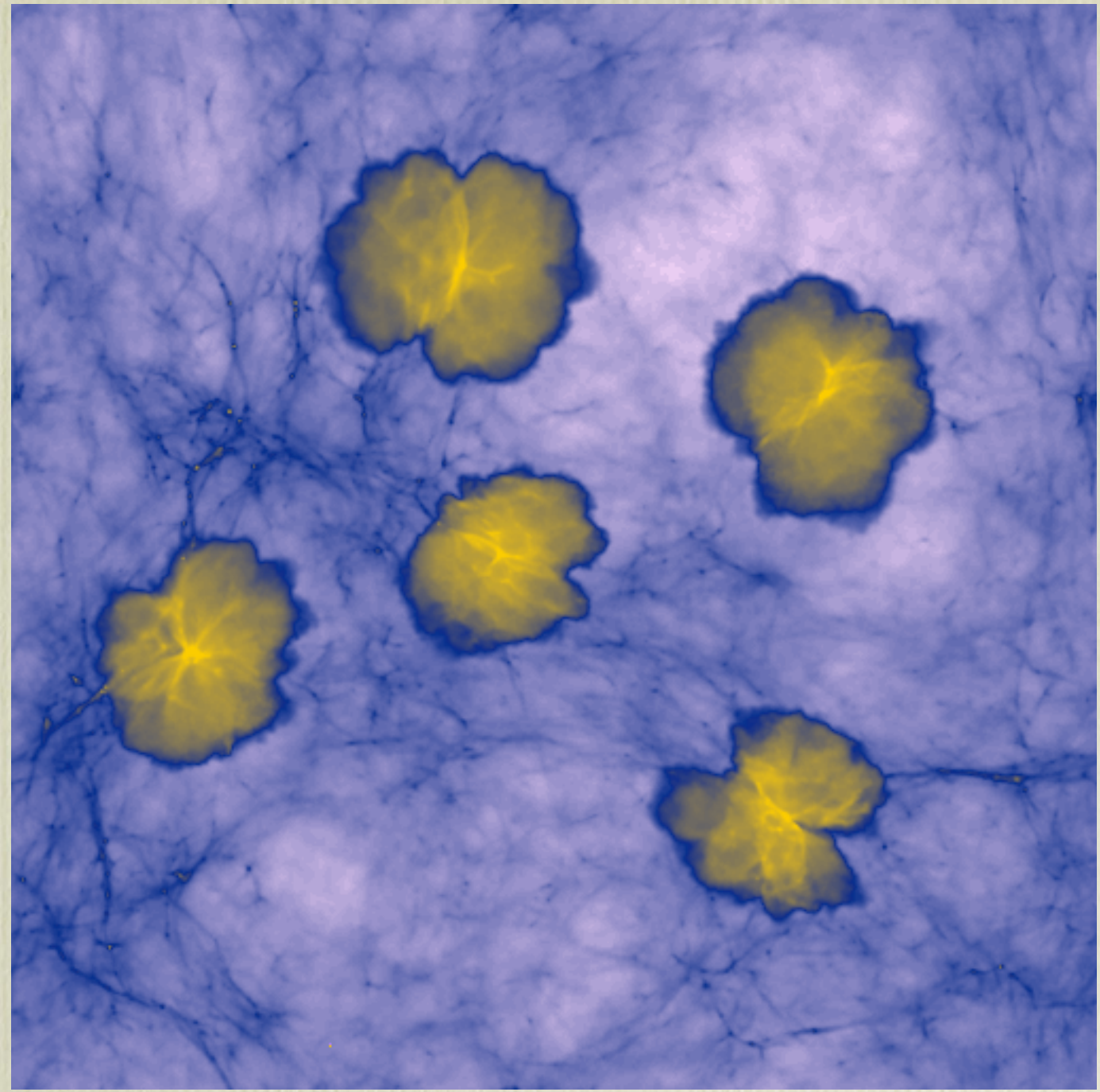

Yoshida et. al.

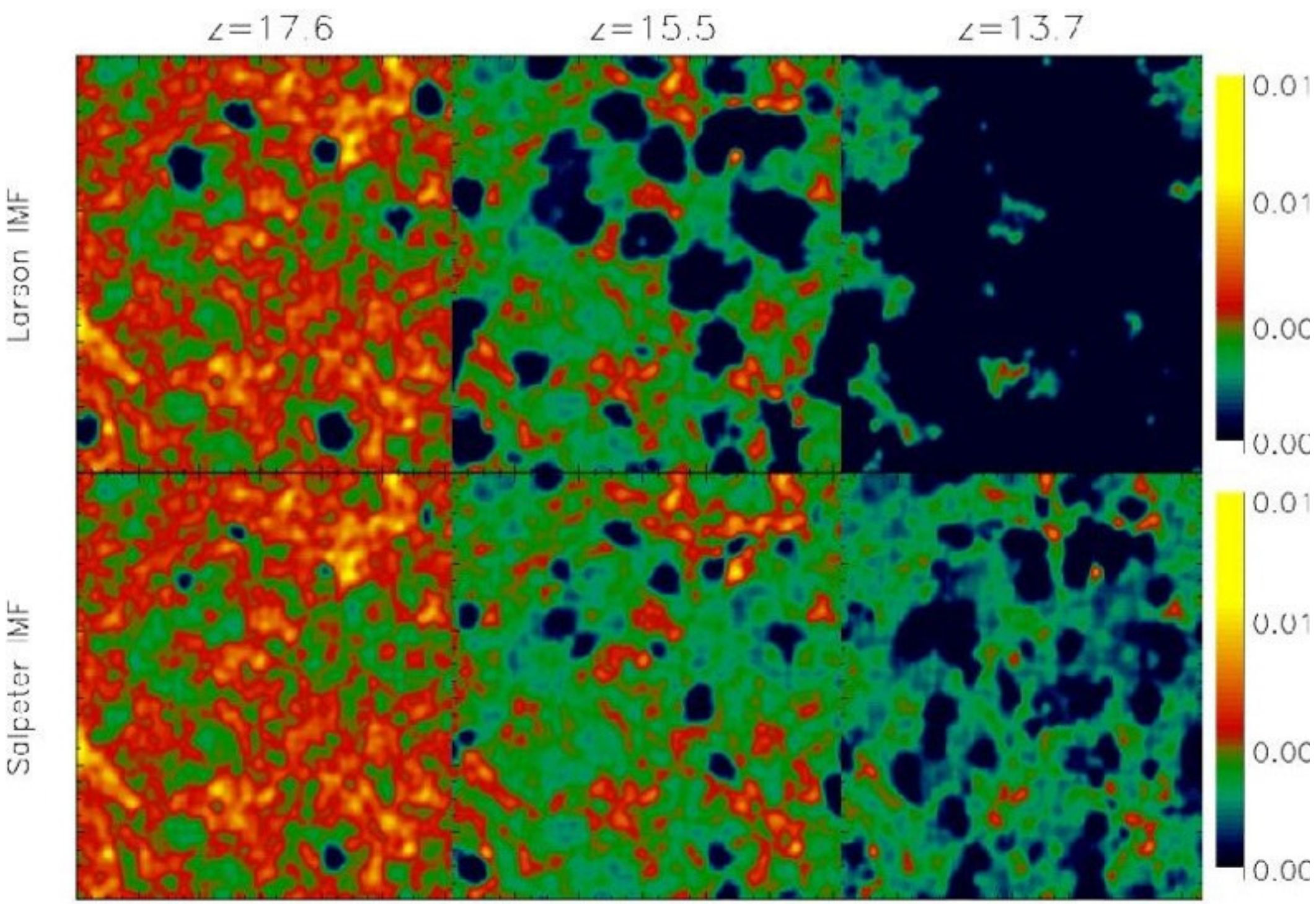

HI number density (Ciardi, Ferrara & White 03)

The Epoch or Reionization: results from detailed modeling

Refs: Benson, Sugiyama, Nusser & Lacey 05; Ciardi, Ferrara & White 03

$f_{esc}=1$ & ~~standard SN feedback~~

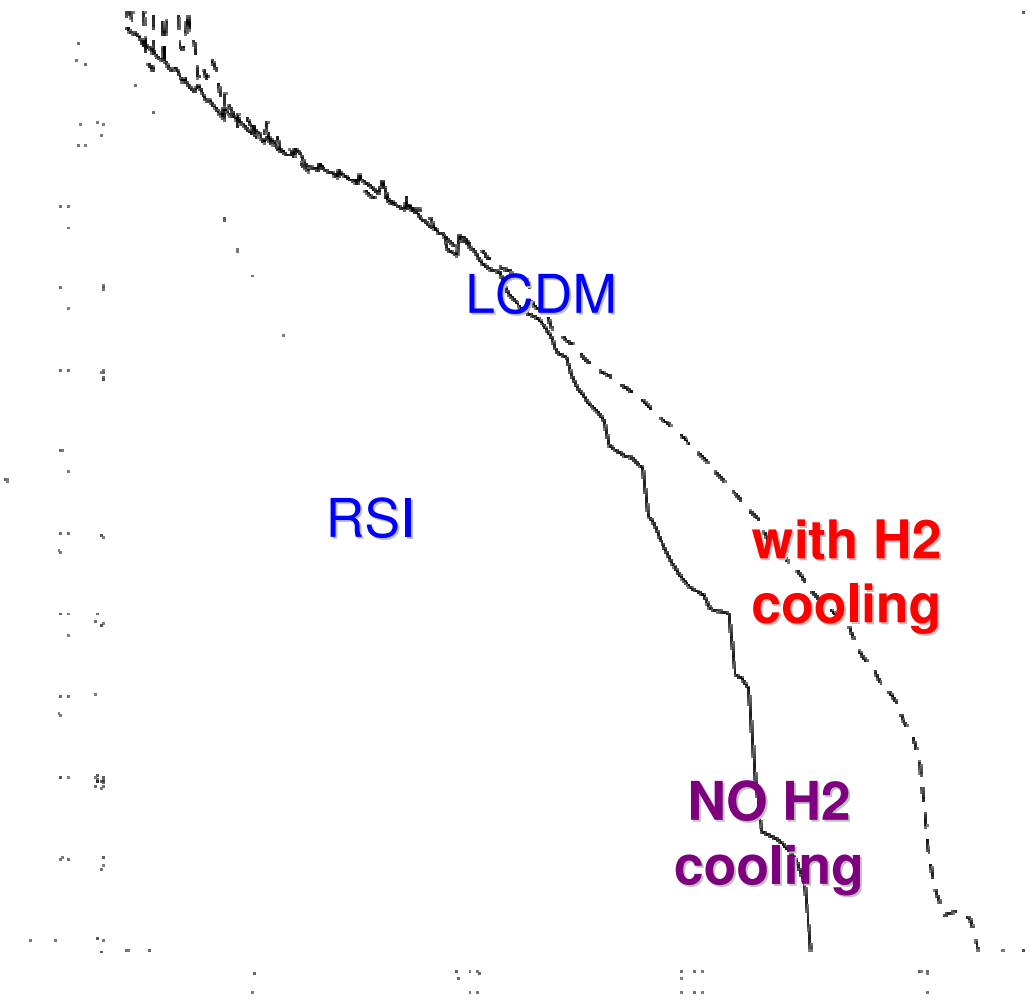

Why is SN feedback important? Only 100 SN explosions can blow away all the gas in a $10^9 M_\odot$ halo with $T_{vir} = 10^4$ K!

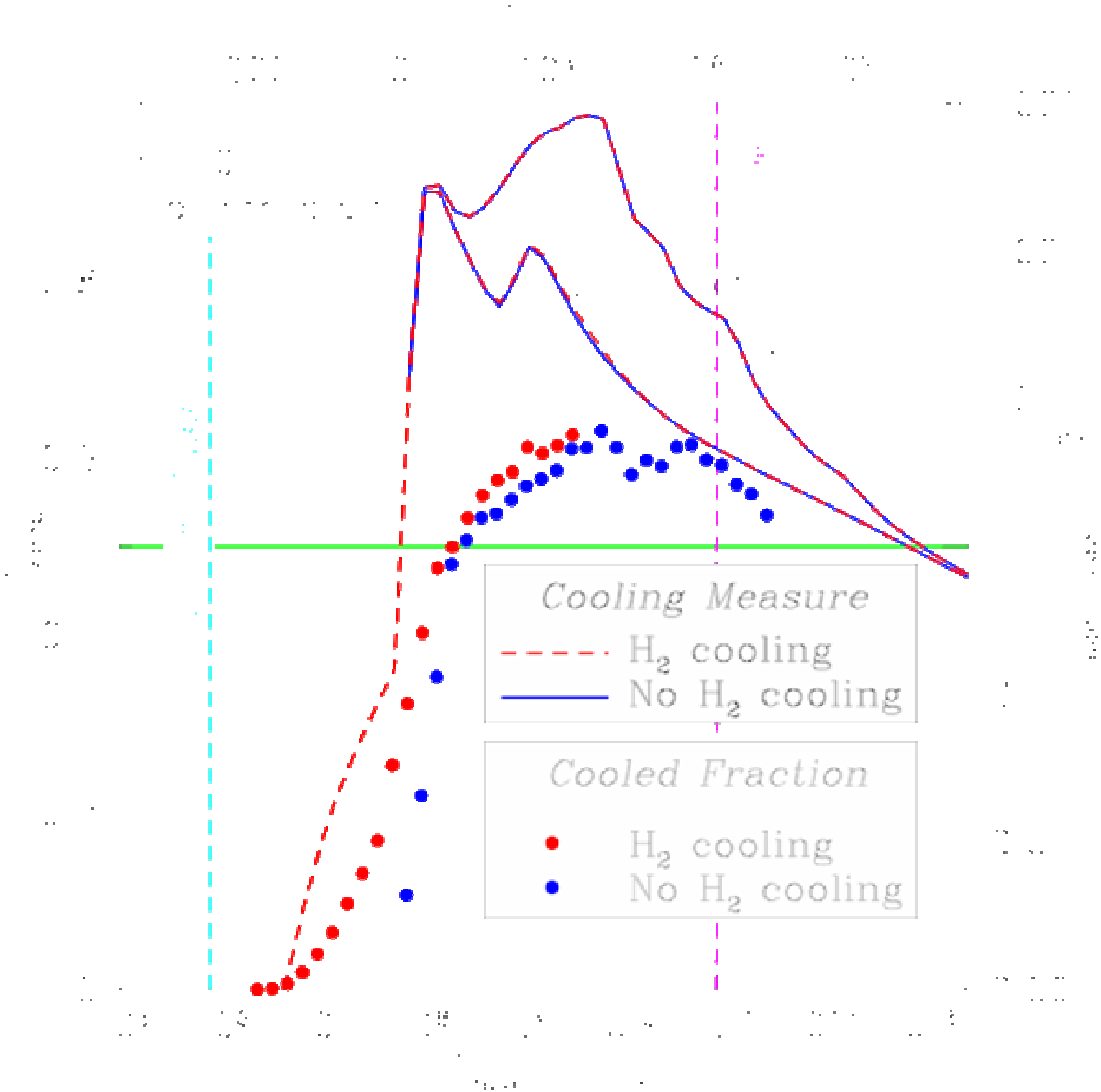
Cooling Measure
H2 cooling
No H2 cooling
Cooled Fraction
H2 cooling
No H2 cooling

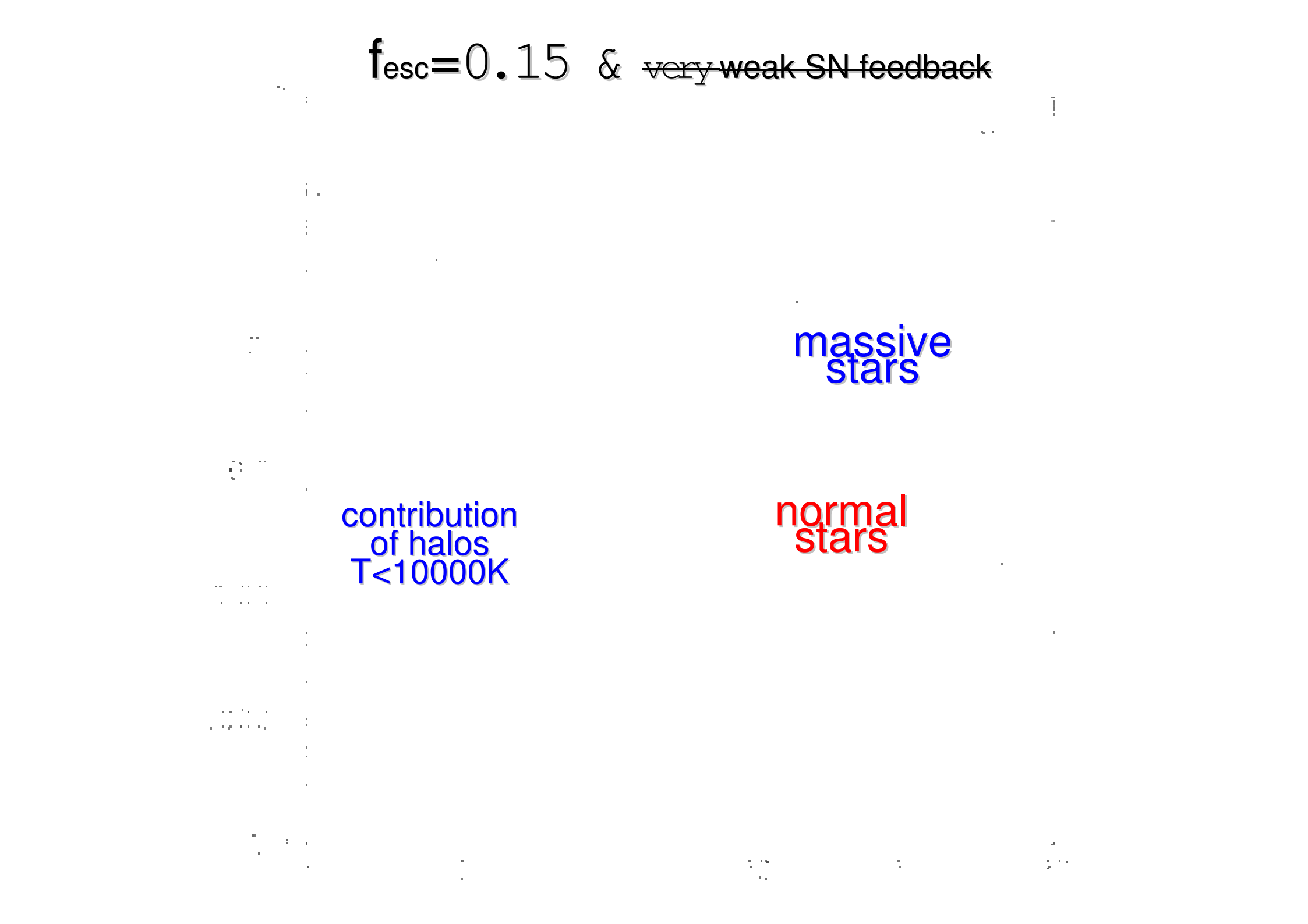
f_{esc}=0.15 & ~~very~~ weak SN feedback
massive stars
normal stars
contribution of halos T<10000K

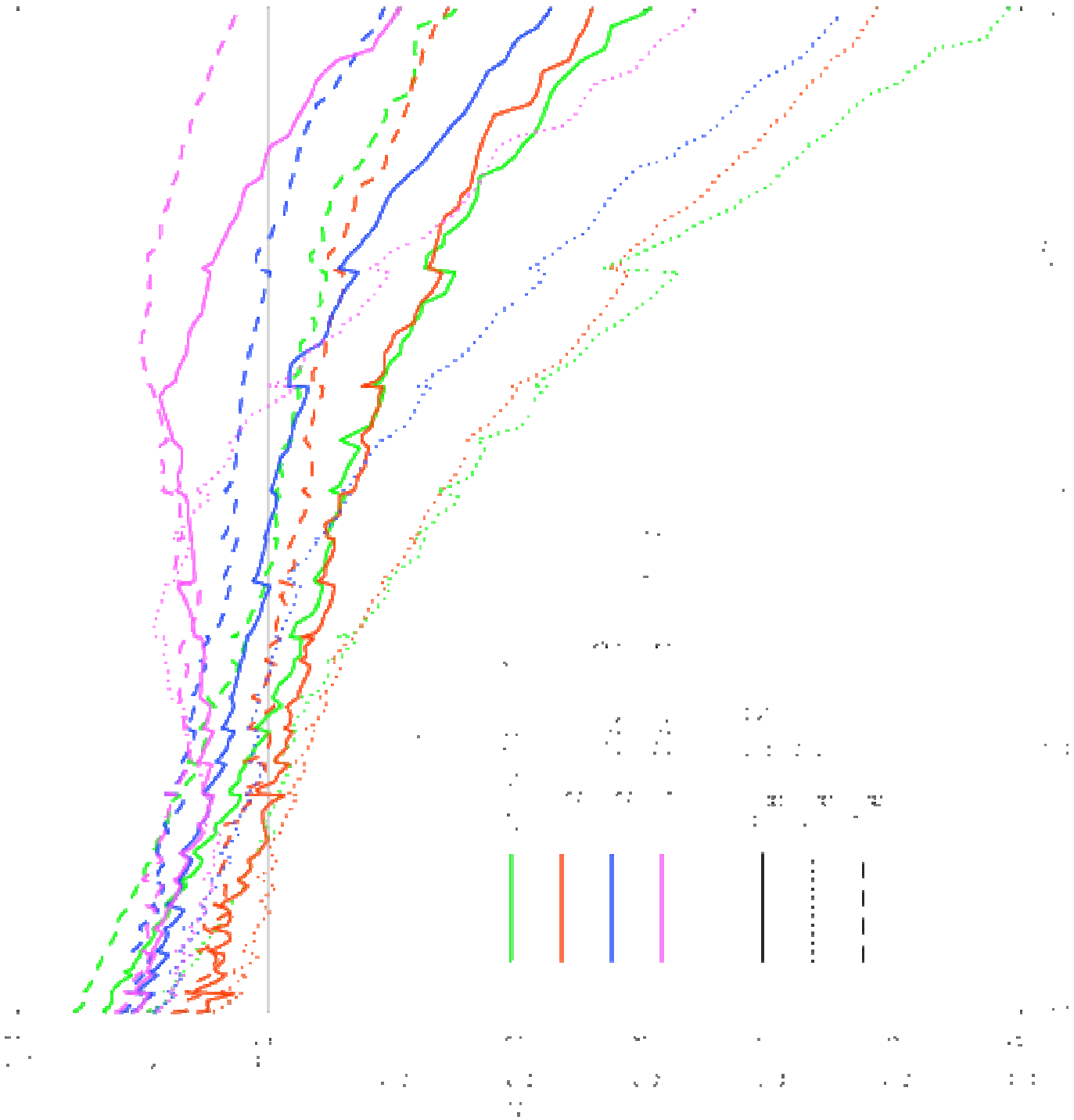

Summary of results

- many models give $\tau \lesssim 0.1$ for high $f_{\rm esc} = 1$ or very weak SN feedback.
- H_2 cooling with standard SN feedback has little effect.
- only models with very weak SN feedback and massive first stars give double reionization: large τ while being consistent with the patchy reionization as indicated by QSO spectra.
- CMB secondary anisotropies can distinguish between some of the scenarios.

Statistical measures of H_I distribution during reionization

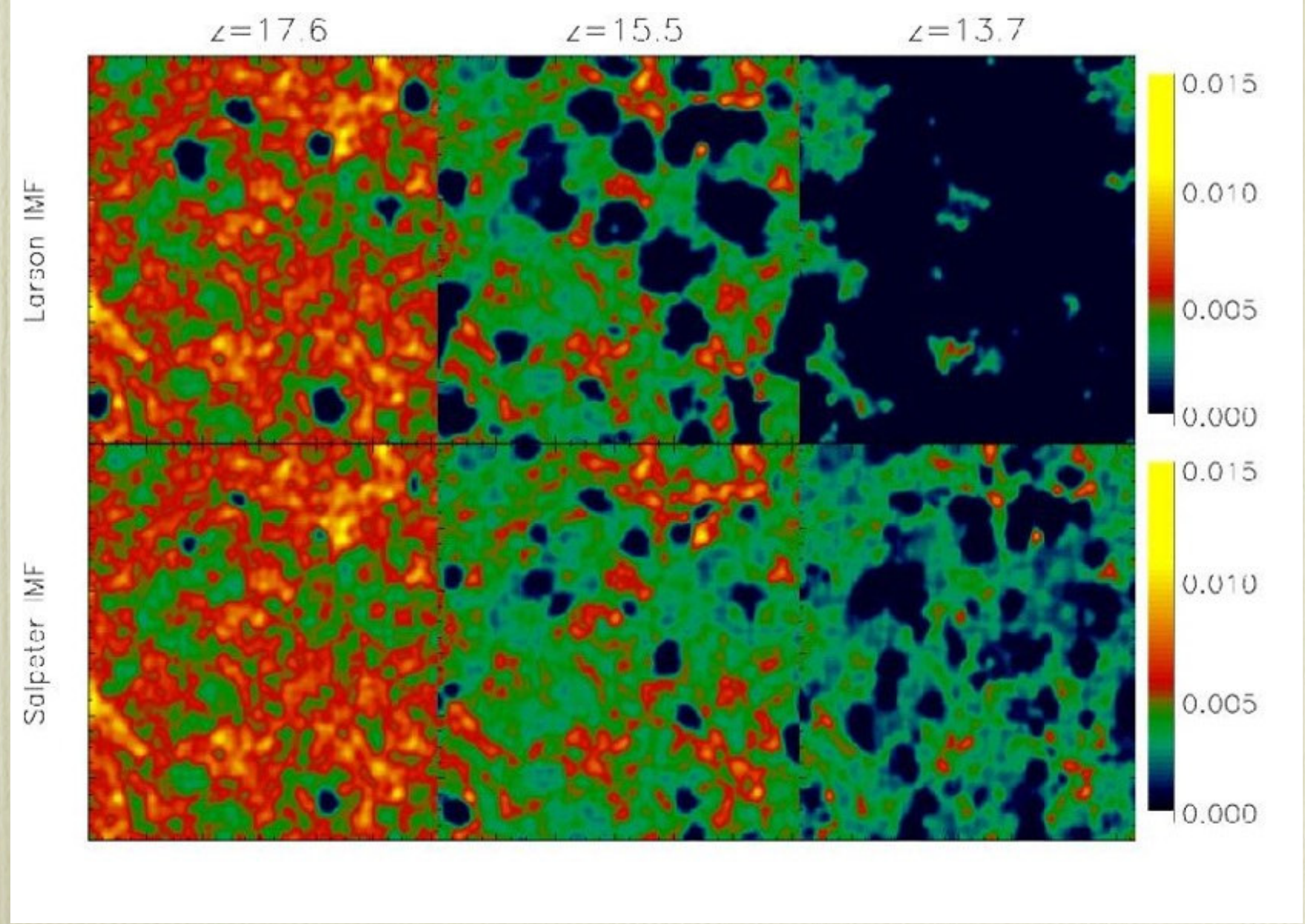

correlation functions, $< n(\mathbf{x})n(\mathbf{x}-\mathbf{y}) >_{\mathbf{x}}$, provide no information about the morphology

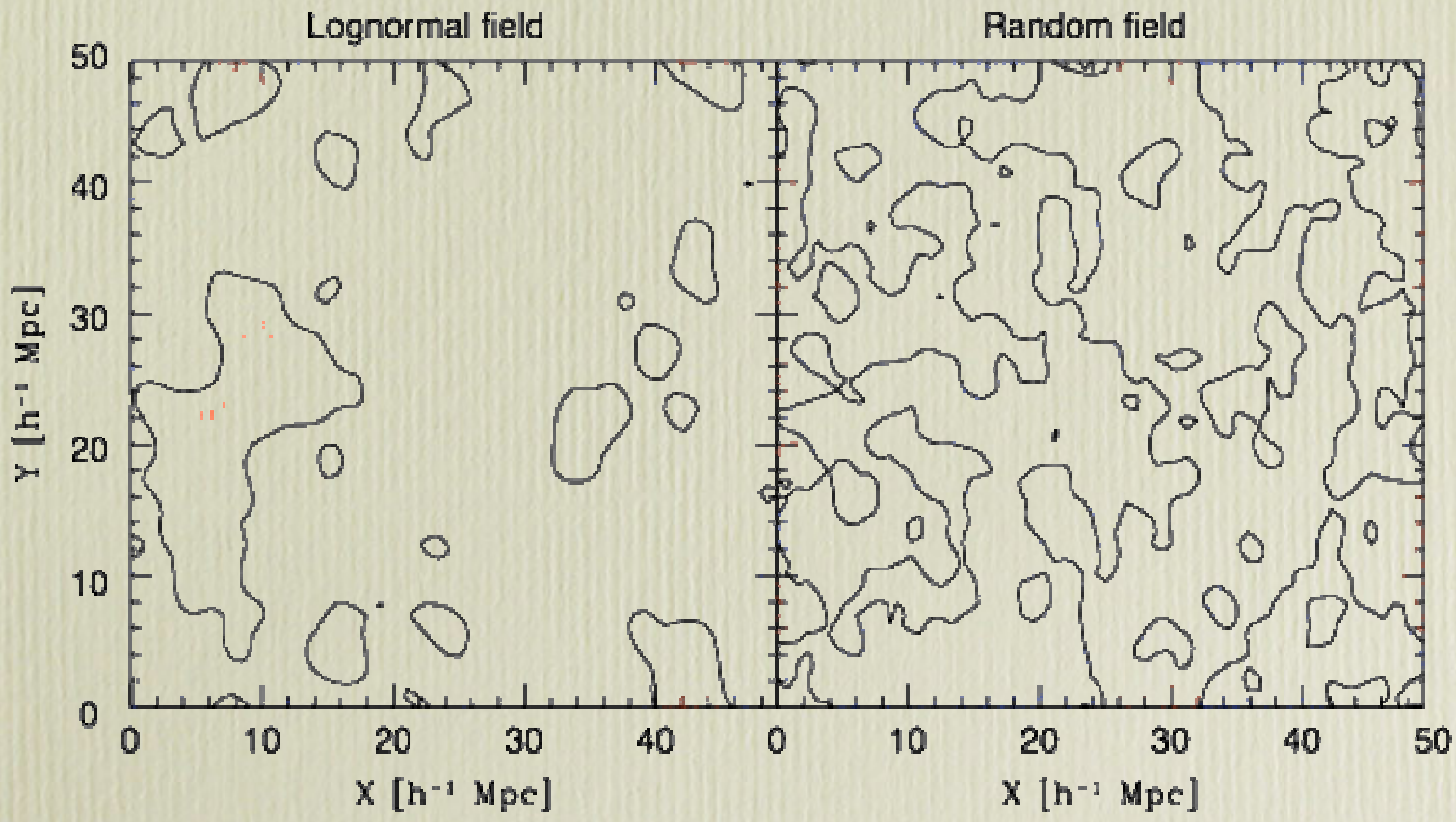

Minkowski Functionals

Minkowski Functionals provide full information on the global topology of objects

For any object:

- M_0 = volume of the object
- M_1 = surface area
- M_2 = mean curvature over the surface
- $M_3 = \chi$ = the Euler characteristic

The Euler characteristic and the Genus

$$2\pi\chi = \int \frac{1}{R_1 R_2}\,\mathrm{d}A$$

This gives $\chi = 2$ for the surface of a sphere, a cube, a pyramid, a potato, a carrot ...

The genus is defined by $\chi = 2(1-g)$

The genus gives the number of holes in an object and is not additive. For a sphere: $g = 0$, $\chi = 2$ For a torus: $g = 1$, $\chi = 0$ For two separate spheres: $g = -1$, $\chi = 4$

$g - 0, \chi - 2$

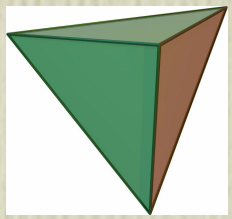

$g - 0, \chi - 2$

$g - 1, \chi - 0$

$g - 0, \chi - 2$

$g - 0, \chi - 2$

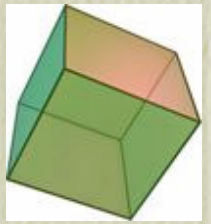

$g - -1, \chi - 4$

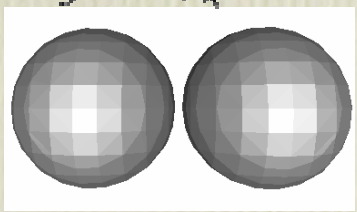

How do we define MFs for $u(\mathbf{x})$?

Let $< u >_V = 0$ & $\sigma^2 = < u^2 >_V$.

The *excursion set* $F_{\tilde{u}}$: all points, $\mathbf{x}$, with $u(\mathbf{x}) \geq \tilde{u}$.

The MFs as a function of $\tilde{u}$ are

$$
\begin{aligned}
V_0(\tilde{u}) &= \frac{1}{V}\int_V \mathrm{d}^3x\Theta\left(\tilde{u}-u(\mathbf{x})\right), \\
V_1(\tilde{u}) &= \frac{1}{6V}\int_{\partial F_{\tilde{u}}} \mathrm{d}^2S(\mathbf{x}), \\
V_2(\tilde{u}) &= \frac{1}{6\pi V}\int_{\partial F_{\tilde{u}}} \mathrm{d}^2S(\mathbf{x})\left[\frac{1}{R_1(\mathbf{x})}+\frac{1}{R_2(\mathbf{x})}\right], \\
V_3(\tilde{u}) &= \frac{1}{4\pi V}\int_{\partial F_{\tilde{u}}} \frac{\mathrm{d}^2S(\mathbf{x})}{R_1(\mathbf{x})R_2(\mathbf{x})},
\end{aligned}
$$

where Θ is the step function.

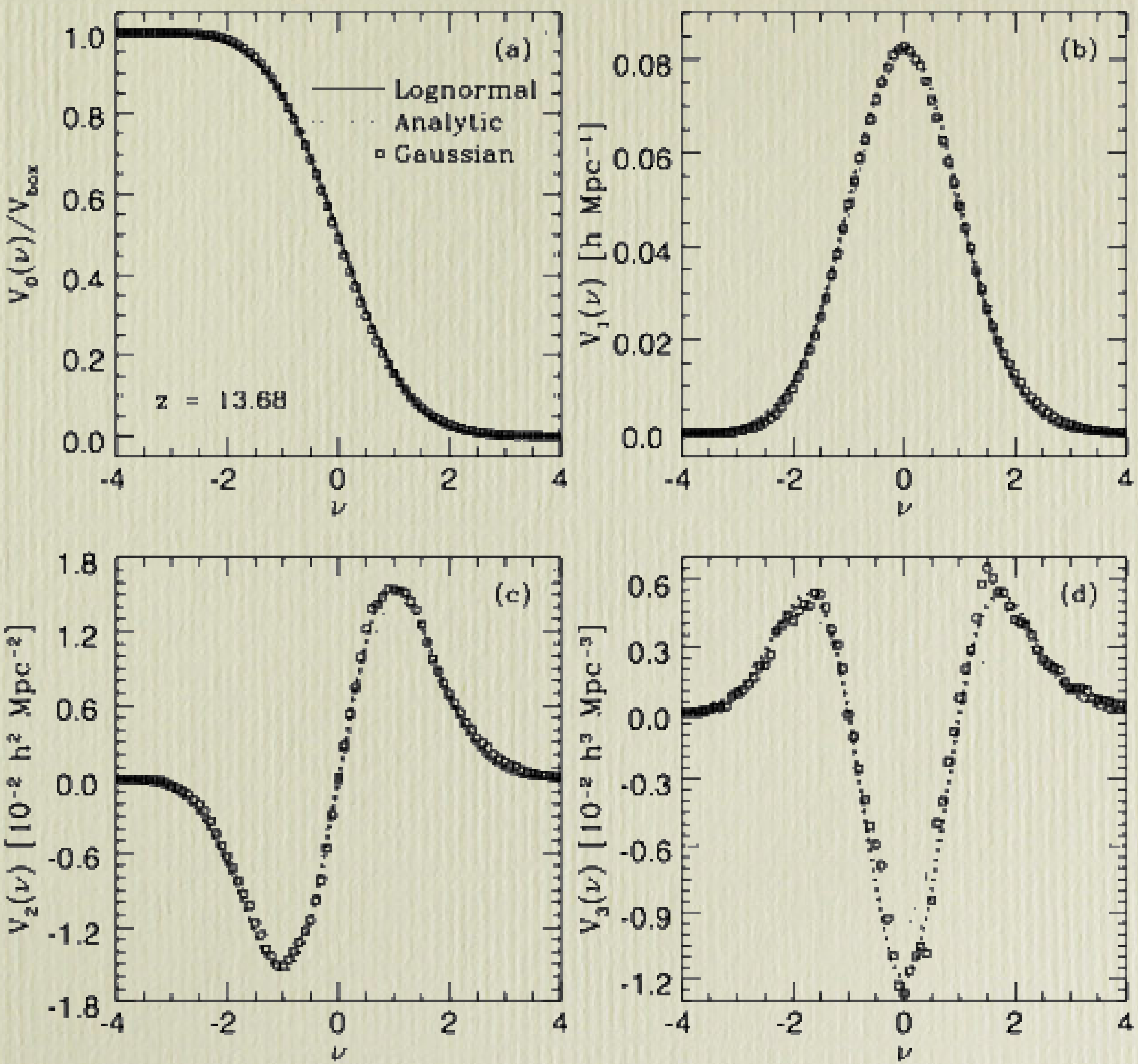
(a)
Lognormal
Analytic
Gaussian
z = 13.68
$V_0(\nu)/V_{box}$
(b)
$V_1(\nu)$ [h Mpc^{-1}]
(c)
$V_2(\nu)$ [10^{-2} h^2 Mpc^{-2}]
(d)
$V_3(\nu)$ [10^{-2} h^3 Mpc^{-3}]
ν

Figure 2. [illegible]

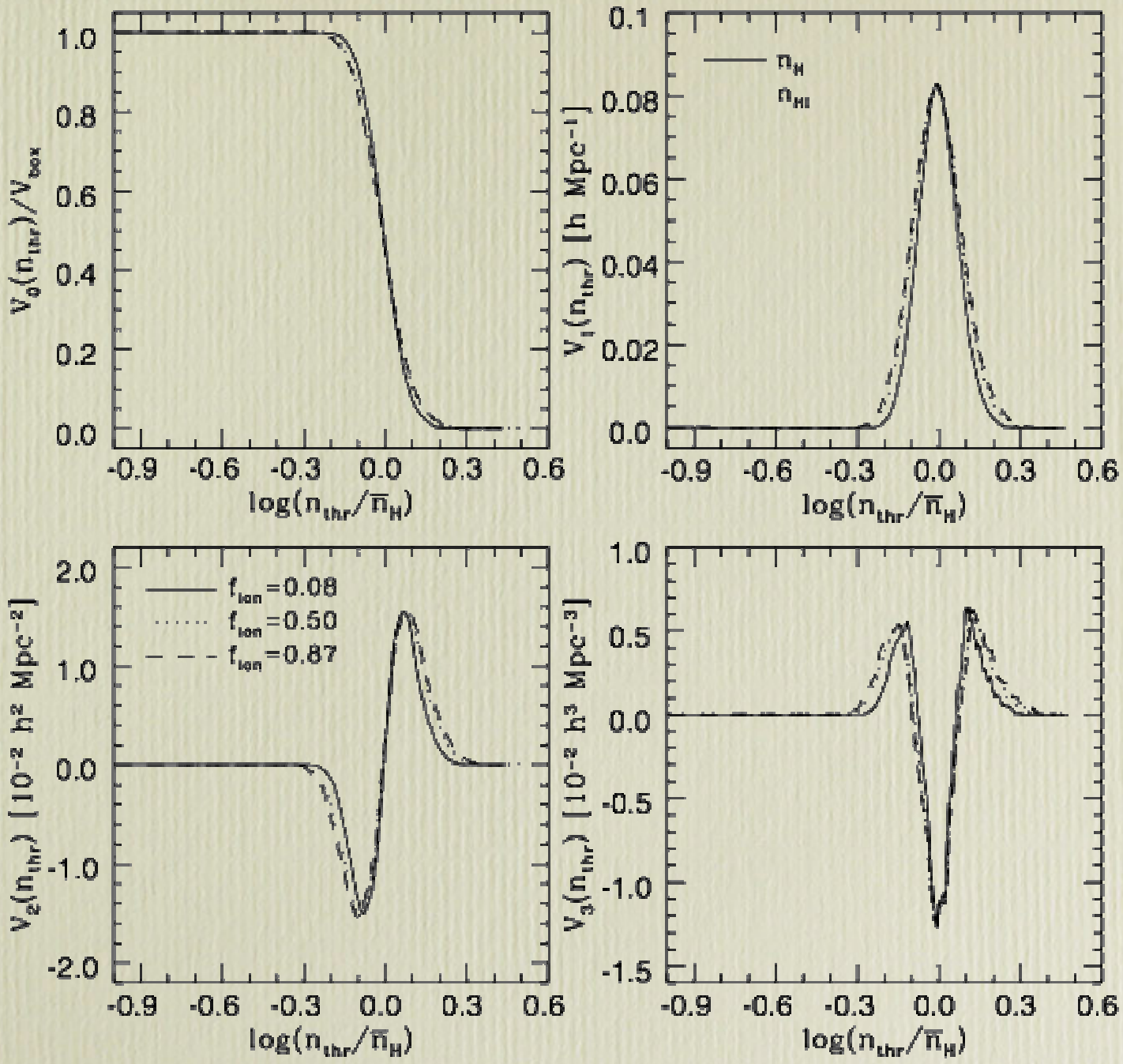

Figure 8. The MFs of the matter (solid lines) and HI (thin lines) isosurface densities in the realization. The box and HI density fields are smoothed with a Gaussian window of 0.5 h^{-1} Mpc in width. Shown are results for neutral fractions of f_{ion} = 0.08 (solid lines), 0.50 (dotted lines), and 0.87 (dashed lines), corresponding to mass weighted mean ionization fractions of $\langle x_i \rangle$ = 0.05, 0.5, and 0.87, respectively.

Probes of reionization

- CMB secondary fluctuations
- spectra of QSOs
- 21 cm from neutral hydrogen during reionization

What is the 21 cm radiation?

Refs: e.g. Field 58

A transition between the two hyperfine states of the ground level of hydrogen. The probability for spontaneous decay is $A_{10} = 2.85 \times 10^{-15}\mathrm{s}^{-1}$ corresponding to a lifetime of 11Myr. This long lifetime is the reason why collisions can be important for establishing a population of triplet. It also makes the line narrow to be observed.

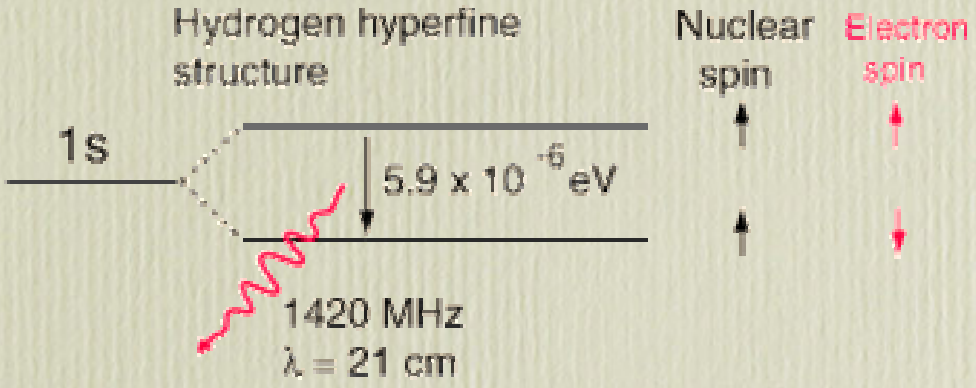

Comparison with Lyα forest

- The 21 cm forest can also be produced in the spectrum of a distant bright object. But the 21 cm "forest" can be seen in emission!

  Why? $h\nu_{\alpha}/kT \sim 10$, while $h\nu_{2,1}/kT \ll 1$.

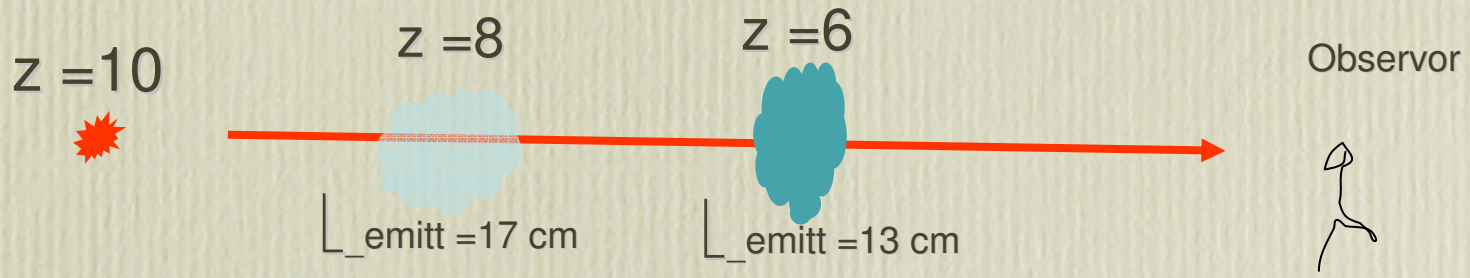

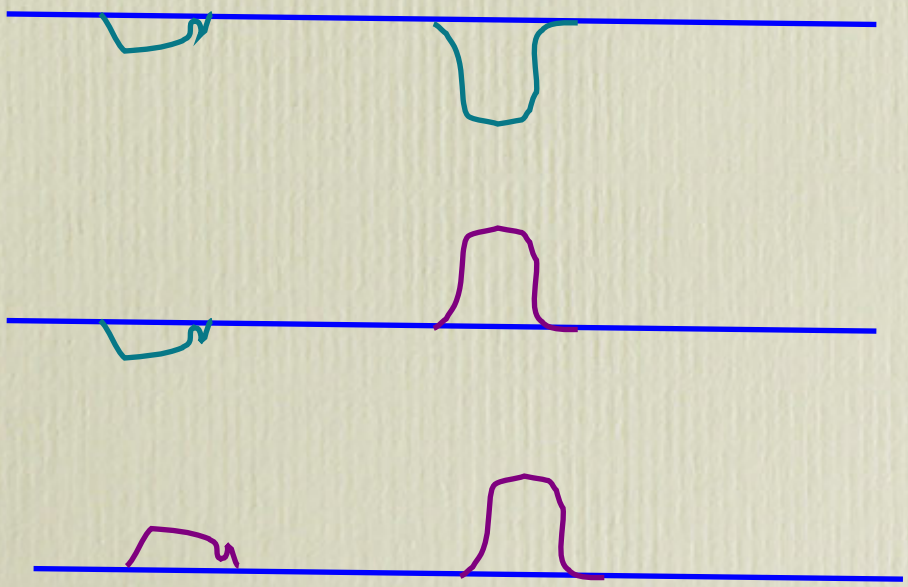

Comparison with Lyα forest

- The 21 cm forest can also be produced in the spectrum of a distant bright object. But the 21 cm "forest" can be seen in emission!

  Why? $h\nu_{\alpha}/kT \sim 10$, while $h\nu_{21\,\mathrm{cm}}/kT \ll 1$.

- For 21 cm we do not need a bright object. We can do a lot better: we can use the CMBR $\Rightarrow$
  - three-dimensional maps of H: distribution!
  - map H: to very high redshifts (but contamination gets more serious)

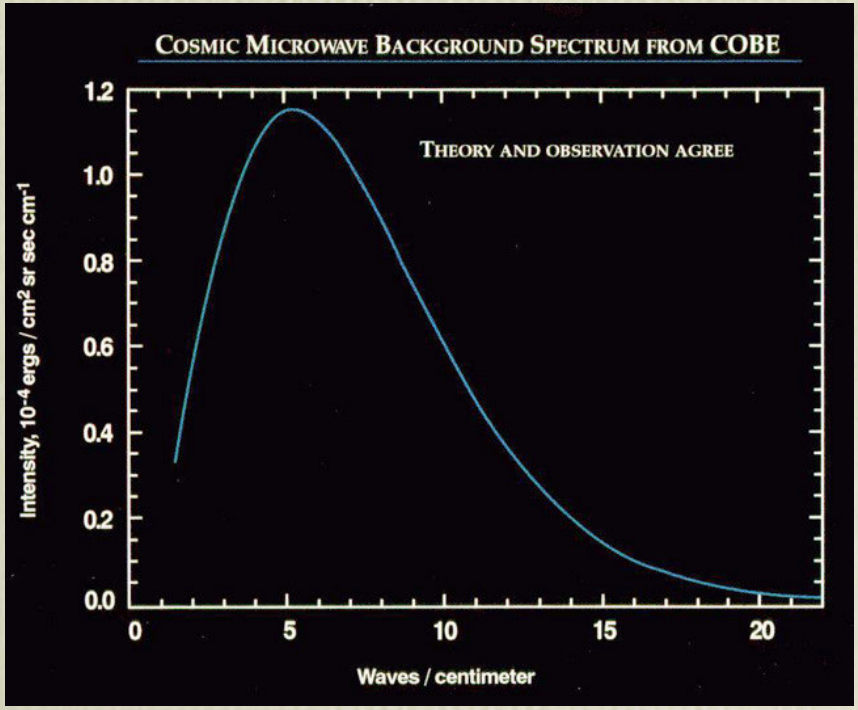

$$\frac{\#of\ triplet}{\#of\ singlet} = 3\exp\left(-\frac{0.068\mathrm{K}^{\circ}}{\mathrm{T_{spin}}}\right)$$

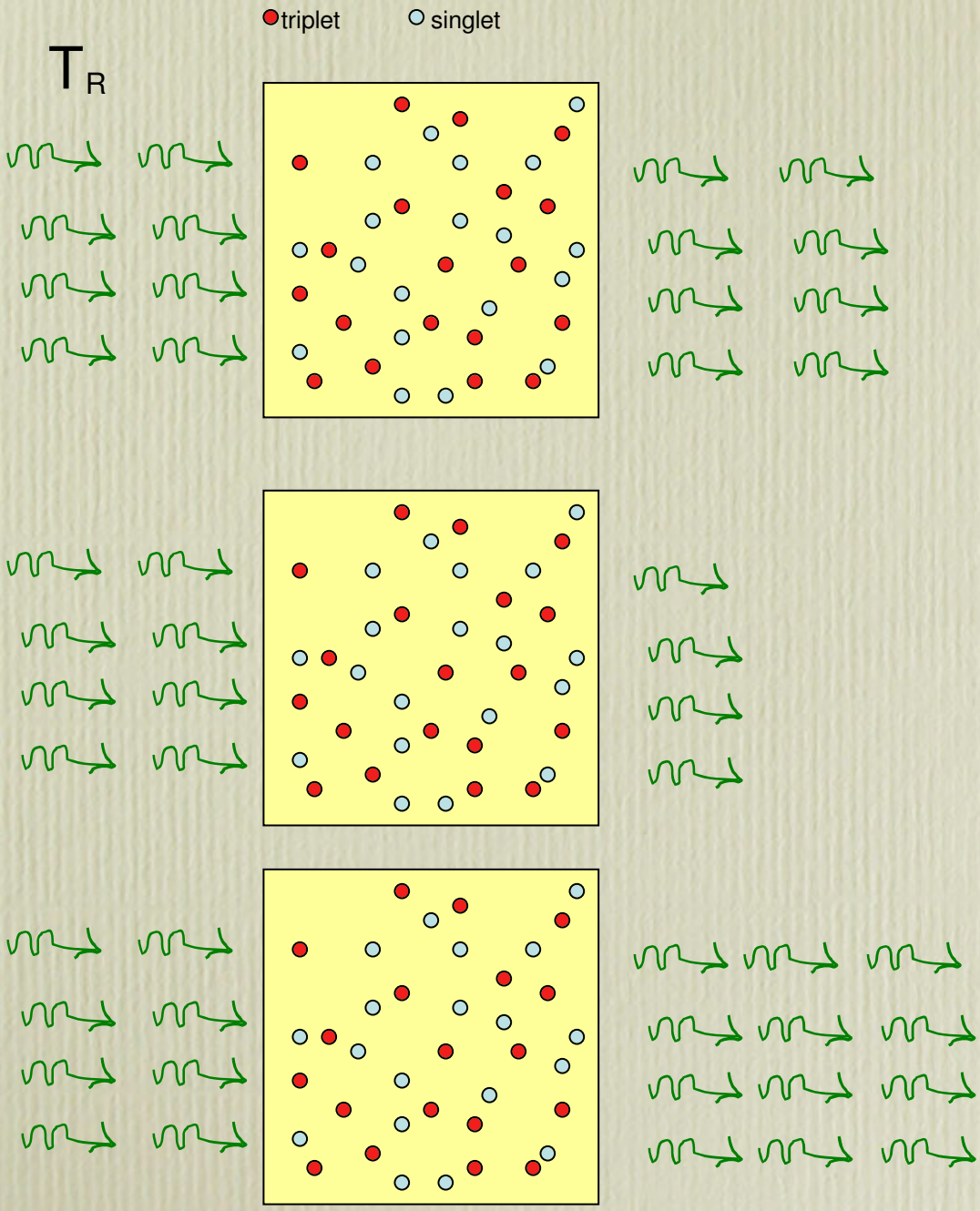

$T_R = T_{spin}$

$T_R > T_{spin}$

$T_R < T_{spin}$

COSMIC MICROWAVE BACKGROUND SPECTRUM FROM COBE

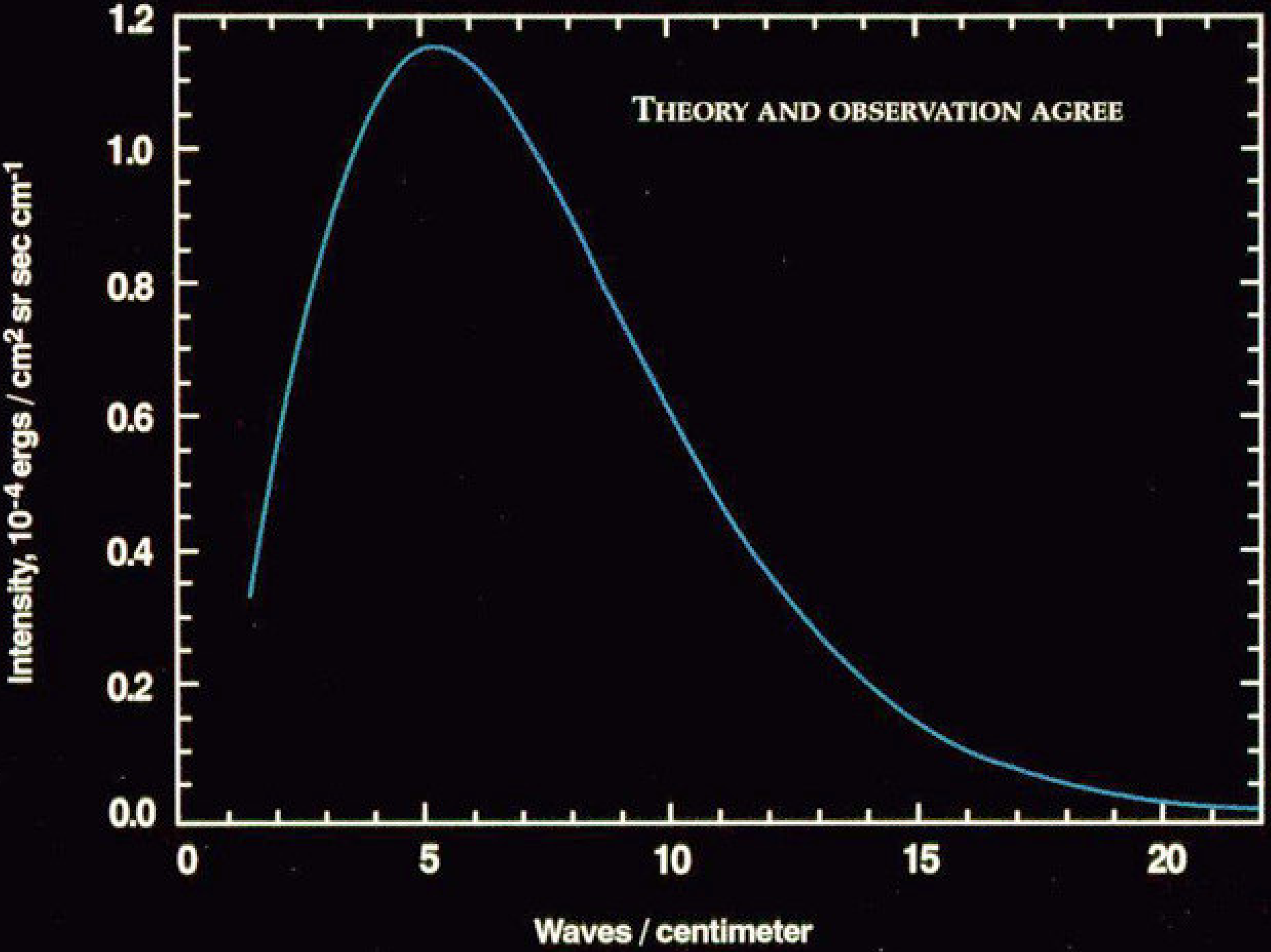

The spin temperature

$$\frac{n_1}{n_0} = 3 \exp\left(-\frac{0.068\mathrm{K}^\circ}{T_s}\right)$$

The spin temperature is determined by

- The CMBR: $\Rightarrow T_s = T_{CMB}$ on a time-scale of 10^4 Yr
- Ly-α pumping: $\Rightarrow T_s = T_K$
- collisions: $\Rightarrow T_s = T_K$

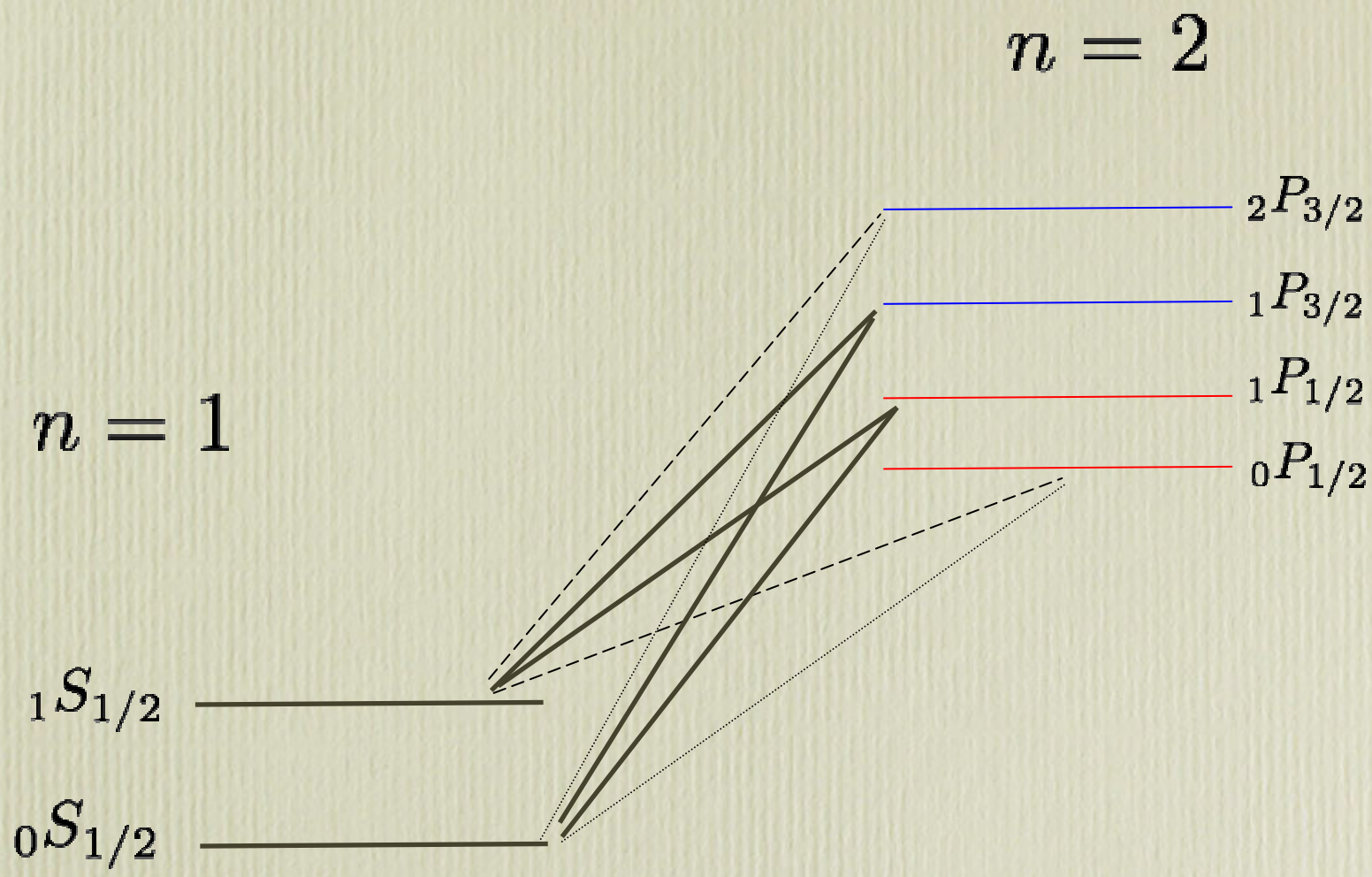

Atomic notation: $_F L_J$

$$\delta T_b \simeq 0.016\ \mathrm{K} \left(1 - \frac{T_{\rm CMB}}{T_S}\right) (1+\delta)(1-x)\left(\frac{\Omega_b h^2}{0.02}\right)\left[\left(\frac{1+z}{10}\right)\left(\frac{0.3}{\Omega_m}\right)\right]^{1/2}$$

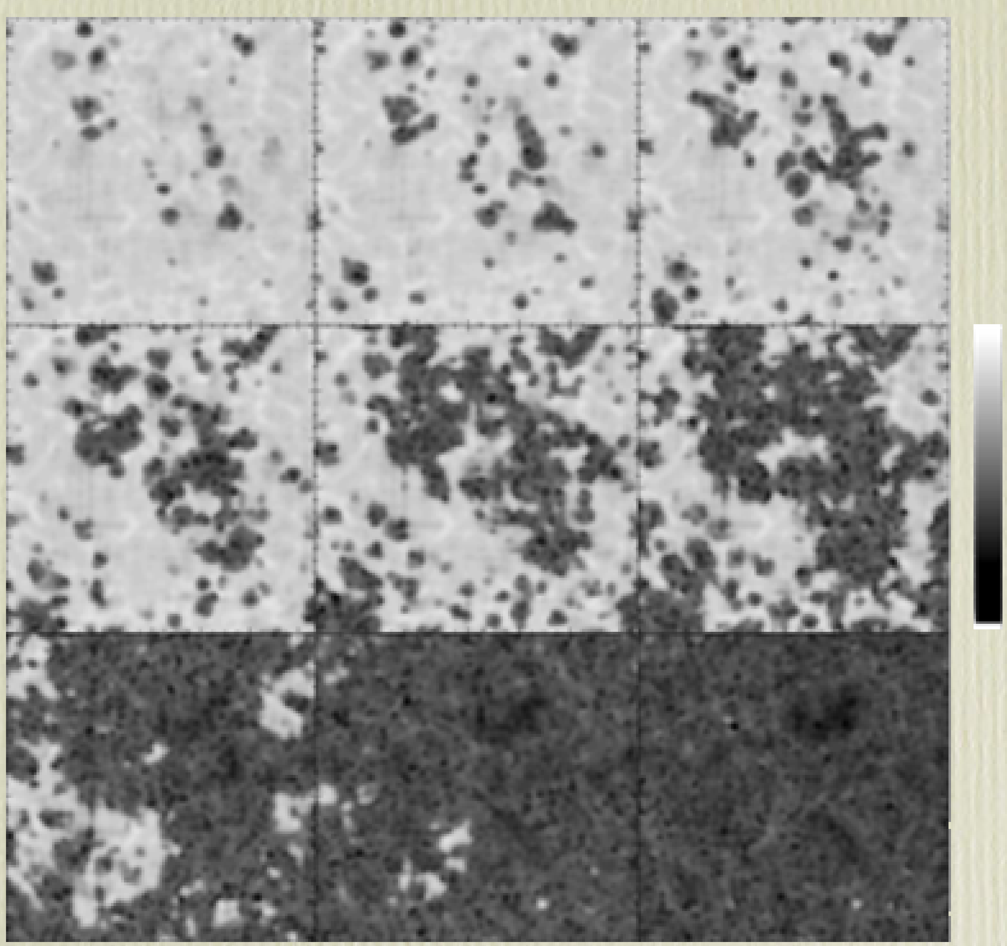

FIG. 3.— Slices through the simulation box in the late reionization model. The nine panels show the differential antenna temperature log δT_b (K) at redshifts (top to bottom and left to right) $z =$ [illegible]. The maps refer to the emission produced by a slice of gas of comoving thickness [illegible] 220 [illegible]

CIARDI & MADAU 2003

Decoupling T_s from T_{CMB} by Collisions

Refs: Field 1959; Allison & Dalgarno 69; Nusser 2005

For fully neutral gas, collisions are only important in high density regions, e.g. H_I in halos (e.g Iliev et. al.02).

For ionized fractions of $x_e \sim 0.1$, collisions are important in moderate density regions. Why? A. larger speed of electrons (relative to atoms) & B. the electric charge of electrons.

Local ionized fractions of $x_e \sim 0.1$ are obtained in x-ray pre-reionization scenarios.

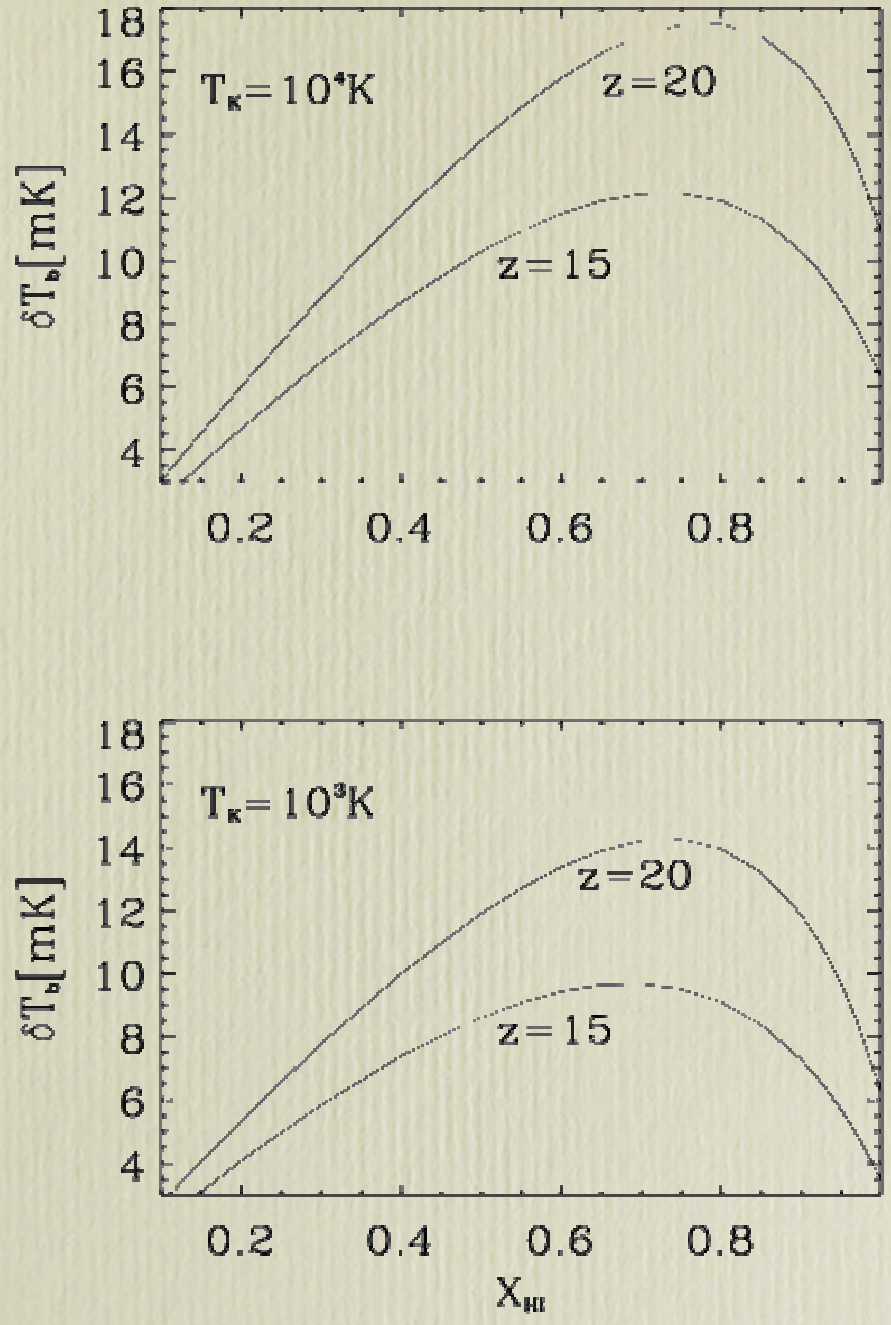

Figure 2. *Top*: The spin temperature at mean density as a function of the neutral fraction x_{HI} for $T_K = 10^4$ K at redshifts $z = 15$ and 20 as indicated in the figure. *Middle*: The DBT at mean density as a function of x_{HI} for $T_K = 10^4$ K. *Bottom*: The DBT for 10^3 K.

x-ray pre-reionization scenarios

Refs: Ricotti & Ostriker 2004

Before UV photons emitted by stars became dominant, X-rays ($E \sim \gtrsim 1$ keV) from gas accreting on intermediate black holes could be important.

X-rays versus UV

- X-rays are less efficient at ionization since most of the energy goes into heating for $x_e \lesssim 0.2$.
- because of the small ionization cross section ($\sigma_i \sim E^{-3}$), an X-ray has a large mean free path $\Rightarrow$ X-ray background.
- to achieve a mean ionization fraction of 50%, one needs 6.8×10^{-6} of the baryons to be accrete on BHs, compared to 4×10^{-4} for UV from stars alone.

Why?

a star's luminosity is 10^{-3} of Eddington's, while a BH's is close to Eddington's.

X-rays easily leak out of high density regions into voids where recombinations are not important.

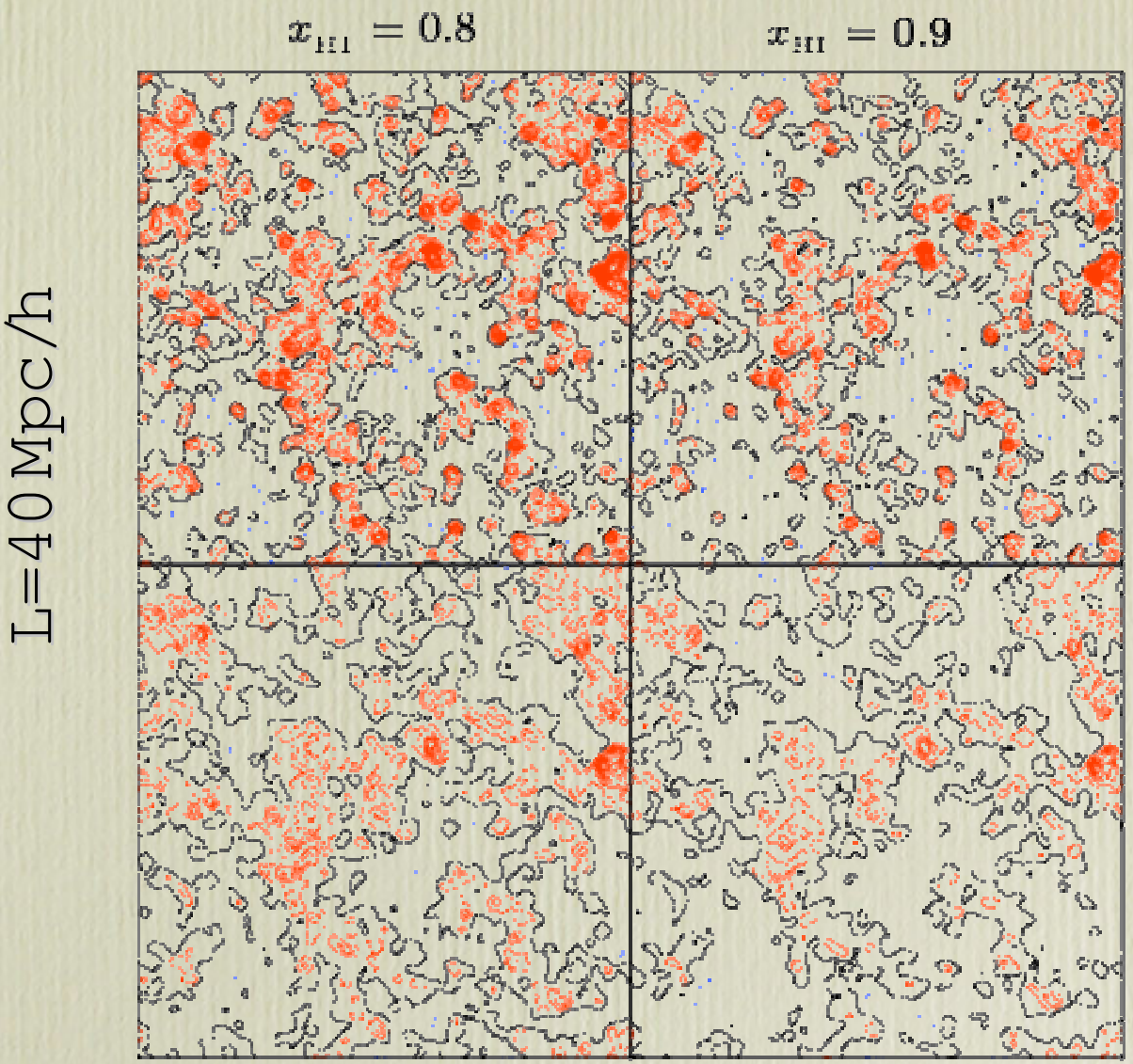

Figure 5. Contour map of the fluctuations in the DBT estimated from the gas density field with σ_8 1 at z 15. The panels in the left and right columns respectively correspond to $x_{\rm II}$ 0.8 and 0.9 at δ 0. The top and bottom panels are for frequency bandwidth of $\Delta\nu$ 10 KHz and 100 KHz, respectively. The maps are for an angular resolution of 3.4 arcmin and the box size is 40 h ^{1}Mpc on the side. The solid thick line marks the SK level of the DBT. Fluctuations below and above the SK level are represented by the light solid and dotted lines, respectively. The contour spacing is 5 mK.

L=1 Mpc/h

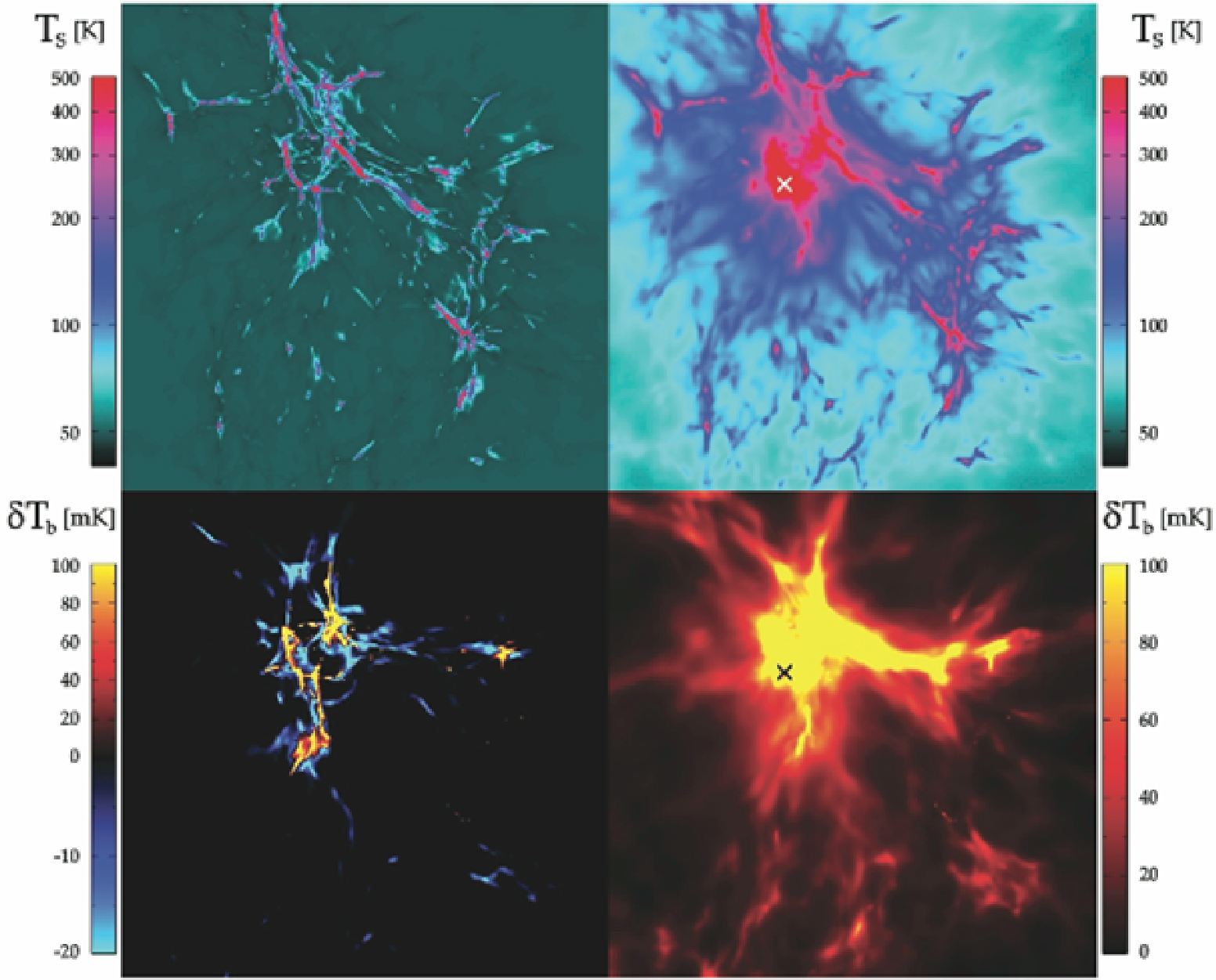

FIG. 2.—Projected (mass-weighted) spin temperature (*top panels*, logarithmic scale) and 21 cm differential brightness temperature (*bottom panels*, composite linear scale) in a 0.5 Mpc simulation box for runs "NoBH" (*left*) and "PL" (*right*) at $z = 17.5$. The location of the miniquasar is indicated by crosses in the right panels.

KUHLEN, MADAU, & MONTGOMERY , 2006

Final remarks

- the prospects for detecting cosmological 21 cm are good. The LOFAR experiment (25000 antennas covering an area of 350km in diameter) might detect 21 cm from $z \lesssim 10$.

High Band Antenna - 120-240 MHz.

Low Band Antenna- 30-80 MHz.

But, No One awes Humanity Anything: foreground contamination could make it impossible to detect reionization in 21 cm.

- where are the ionizing galaxies?